3D-Printed Inflatable Actuators

Design and Development of Soft Actuators for a Pneumatically-Actuated Soft Robotic Arm

Eidgenössische Technische Hochschule Zürich
Swiss Federal Institute of Technology Zurich

Institute for Dynamic Systems and Control
IDSC
Institut für Dynamische Systeme und Regelungstechnik

Hong Fai Lau

3D-Printed Inflatable Actuators

Design and Development of Soft Actuators for a Pneumatically-Actuated Soft Robotic Arm

Semester Project

Institute for Dynamic Systems and Control
Swiss Federal Institute of Technology (ETH) Zurich

Supervision

Matthias Hofer
Prof. Dr. Raffaello D'Andrea

August 2019

IDSC-RD-MHo-02

Abstract

Designing soft inflatable actuators is not a trivial task due to the coupling between their function and their mechanical design. Hence, in order to realize a functional design, numerous design parameters and their interdependencies have to be studied. As a result, the design process is often both tedious and ambiguous as there is no well-defined approach to guide it. In this semester project, 3D-printed inflatable actuators were designed, analyzed, and realized. The goal of this project is to eventually incorporate them into a pneumatically-actuated soft robotic arm with two Degrees of Freedom. The bellow-type actuators were systematically developed using a two-phased design process. The linear effects of geometry and material were first studied. The insights from this phase were then translated into the more complex rotational domain using a design framework. It is in the rotational domain where the insights were applied to generate a soft inflatable rotary actuator. At each phase of this design process, Finite Element Analysis simulation and physical experimentation were used to verify the mechanical designs. This structured approach led to the first realization of a soft inflatable rotary actuator that possesses a deflection behavior that is suitable for the envisioned soft robotic arm.

Keywords: Soft robotics, inflatable actuators, mechanical design, 3D-printing.

Contents

Nomenclature

Acronyms and Abbreviations

CAD	Computer-Aided Design
DoF	Degrees of Freedom
EIA	Elastic Inflatable Actuator
FEA	Finite Element Analysis

Chapter 1

Introduction

Research about soft inflatable actuators has recently gained much attention. The advent of new materials, manufacturing methods as well as simulation tools are responsible for its latest developments [1]. The growing interest in the benefits that these devices promise to bring fuel the demand for new and improved designs. These benefits include but are not limited to the following: i) intrinsically safe physical human-robot interaction [2], ii) fast actuation capabilities [3] and iii) low manufacturing costs [4]. While the need for novel soft inflatable actuator designs is increasing, developing them is unfortunately not a straightforward process. The embedding of the function of these devices into their mechanical design complicates the design process [1]. Hence in order to produce a functional design, one has to carefully explore a design space that is not only high-dimensional but also riddled with complex interdependencies. Thus, the design process is usually both taxing and vague as there are minimal guidelines to follow.

In this semester project, different 3D-printed inflatable actuators were systematically designed, analyzed, and realized. Figure 1.1 shows an example of a 3D-printed inflatable rotary actuator. The primary motivation behind this project was to design a soft inflatable actuator for a pneumatically-actuated soft robotic arm that has two Degrees of Freedom (DoF). The design problem was first simplified into two phases, namely, the linear domain and the rotation domain. Given the limited literature available and the vast design space, it suggests that doing otherwise by arbitrarily designing such an actuator is virtually intractable. In the first phase, the geometry and material of linear bellow-type actuators were studied. The insights gained were subsequently converted into the rotational domain. The eventual soft inflatable rotary actuator was generated using these insights in the rotational domain. Finite Element Analysis (FEA) simulation and physical experimentation were used to verify the mechanical designs. These led to the realization of a soft inflatable rotary actuator that emits high angular deflection at relatively low pressures, hence being suitable for the intended soft robotic arm.

This semester project report covers the entirety of the design process, from the conceptualization to the realization of the 3D-printed inflatable rotary actuator. The organization of the report is as follows: Chapter 2 details the design process as well as reviews existing literature. Chapter 3 covers the simplification of the design problem into the linear domain. Chapter 4 explains how the insights gained from the linear domain are being converted into the rotational domain and subsequently used to generate the mechanical design of the soft inflatable rotary actuator. Last but not least, Chapter 5 concludes the project.

Figure 1.1: The realized 3D-printed inflatable rotary actuator.

Chapter 2

Design Process and Literature Review

The objective of this semester project was to develop a soft inflatable actuator meant for a pneumatically-actuated soft robotic arm with two DoF. The development of this device was a continuation of a previous work where a one DoF soft robotic arm was developed and researched upon [5].

This chapter begins with a review of the latest iteration of the soft robotic arm, in a bid to not only better understand the design problem, but also come up with the design requirements for the eventual soft inflatable actuator. Previously developed soft inflatable actuator designs are subsequently reviewed in order to gain insights regarding these devices. Relevant 3D-printing processes are then briefly touched on. Last but not least, the design approach for the project is explained.

2.1 Design Problem and Requirements

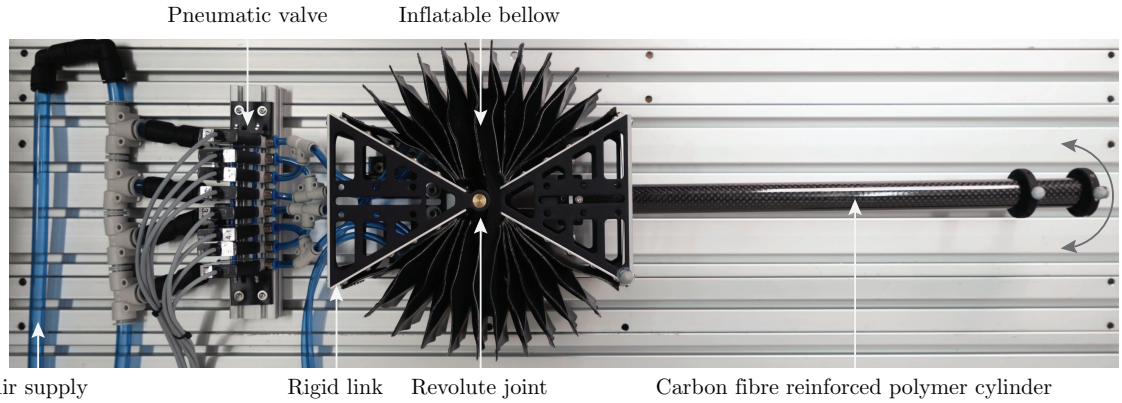

Figure 2.1: Current iteration of the one DoF soft robotic arm.

Figure 2.1 shows the current iteration of the one DoF soft robotic arm. The arm consists of two links that are connected via a revolute joint. Two fabric-based inflatable bellows which are in an antagonistic configuration, actuate the arm. In other words, it is the pressure difference between these two bellows that causes the arm to move. While these bellows fulfill their roles, manufacturing them is both laborious and expensive. In order to make these bellows, polyurethane-coated nylon fabric is high frequency welded by hand. This manufacturing method imposes a considerable constraint on the overall mechanical design of the soft robotic arm. Hence, it is

desirable to explore the idea of 3D-printing these bellow-type actuators. By doing so, not only will it ease the manufacturing process, but it will also enable the realization of more complicated designs such as a two DoF version of this soft robotic arm.

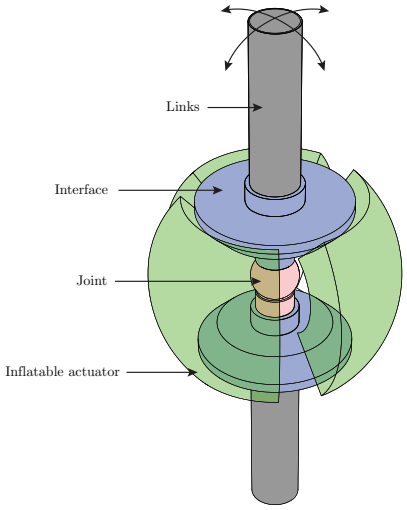

Figure 2.2: Conceptual sketch of the two DoF soft robotic arm.

The two DoF soft robotic arm was conceptualized in order to gain a deeper understanding of the design problem. A sketch of it is shown in Fig. 2.2. Similar to the one DoF version, it is pneumatically-actuated and consists of two links (in grey). Each of these links has its ends terminated with an interface (in blue) where air supply tubes and other essentials will be connected. The interfaces are coupled via a joint (in red), where a magnetic ball joint may be used. Not only will it enable the additional DoF, but it also offers a fixed center of rotation while allowing a large range of motion of the arm. Three inflatable actuators surround the joint and are spaced 120° apart (in green). This configuration is desirable as it requires the least amount of modifications required to be made to the current system infrastructure. Lastly, the two DoF soft robotic arm is desired to be on the same scale as a human arm. With these, the focus of this project will be on the mechanical design of these inflatable actuators as designing one for this purpose is certainly not easy.

Since the performance of the eventual soft robotic arm is dependent on the inflatable actuator, the following design requirements for the latter were formulated in order to guide the design process:

1. Large range of motion: This ensures that a large task space of the soft robotic arm.

2. Actuate under small amounts of pressure: This enables the soft robotic arm to be both fast and safe.

3. Ease of manufacturing: The benefits of fulfilling this is twofold. Not only will it reduce any downtime due to manufacturing or maintenance, but it will also enable more complicated designs to be realized as mentioned above with 3D-printing.

The following point distills the above design requirements: the eventual inflatable actuator has to be both highly compliant and 3D-printed. One more subtle requirement is that the inflatable actuator has to deflect rotationally. With this, the following section reviews previously developed soft inflatable actuator designs, in a bid to understand their underlying mechanisms and assess their applicability to this project.

2.2 Soft Inflatable Actuators

Soft inflatable actuators mark a paradigm shift in the development of actuators. In a typical actuator made from rigid materials, for example, a Series Elastic Actuator [6] or a Variable Stiffness Actuator [7], the schematics, components, and control together define the function of the device. In a soft inflatable actuator, however, its function solely depends on its mechanical design [1]. Hence, the mechanical design plays a pivotal role in soft inflatable actuator development. However, designing these actuators is a complicated task because one has to consider an exhaustive list of parameters such as geometry, material, actuation medium during the design process. Hence, it is common to rely on nature for inspiration [2].

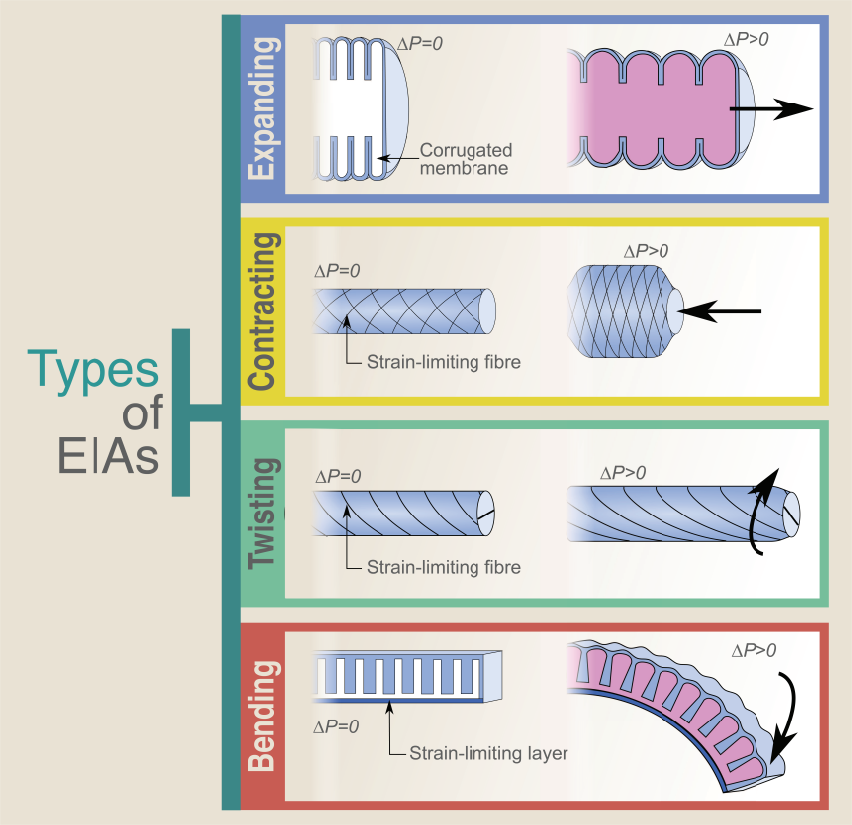

Figure 2.3: Various types of EIAs. Reprinted from Advanced Materials, vol. 29, no. 43, Benjamin Gorissen, Dominiek Reynaerts, Satoshi Konishi, et al., Elastic Inflatable Actuators for Soft Robotics Applications, 2017, with permission from John Wiley and Sons. © 2017, WILEY-VCH Verlag GmbH & Co. KGaA, Weinheim [1]

An extensive literature review showed that there was no existing design that exactly fits the design problem. Despite that, insights were still gained from this study, and they will be detailed below.

Given the design problem, the most promising class of soft inflatable actuators for this project is the Elastic Inflatable Actuator (EIA). As its name suggests, this device actuates under positive pressure. Figure 2.3 [1] gives an overview of the different types of EIAs. It is clear from the figure that the deflection behavior of these devices depends on their mechanical design.

One promising design is a bending-type EIA. While the deflection behavior of this actuator is not entirely applicable, its principle may still be adapted for the eventual mechanical design. A key feature of this design is the idea of asymmetry. Figure 2.4 shows the different kinds of asymmetries

[1] Special thanks to Benjamin Gorissen for providing the source files of this figure.

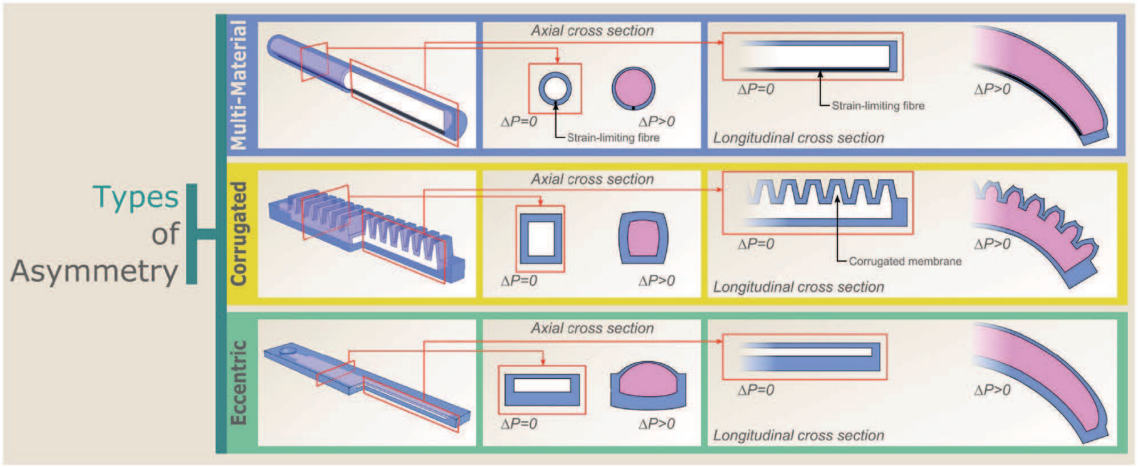

Figure 2.4: Various types of asymmetry embedded into bending-type EIAs. Reprinted from Advanced Materials, vol. 29, no. 43, Benjamin Gorissen, Dominiek Reynaerts, Satoshi Konishi, et al., Elastic Inflatable Actuators for Soft Robotics Applications, 2017, with permission from John Wiley and Sons. © 2017, WILEY-VCH Verlag GmbH & Co. KGaA, Weinheim [1]

that may be present in a bending-type EIA. This type of device relies on asymmetry to bend towards its desired side, which is its stiffer side. This principle is important as it may be extended to any arbitrary deflection behavior.

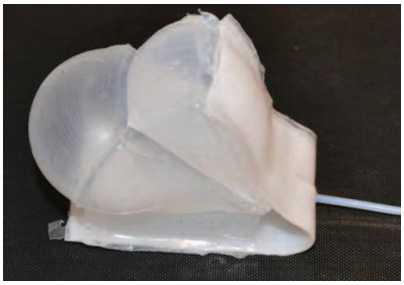

Figure 2.5: Rotary Soft Pneumatic Actuator. Reprinted from IEEE/RSJ International Conference on Intelligent Robotics, pp. 442 – 458, Yi Sun, Yun Seong Song, Jamie Paik, Characterization of silicone rubber based on soft pneumatic actuators, 2013, with permission from IEEE. © 2013, IEEE [8].

The literature review also identified another potential EIA which expands rotationally. It is the Rotary Soft Pneumatic Actuator [8] as pictured in Fig. 2.5. Even though the device only has one DoF, an interesting design feature of this expanding-type actuator is that its center of rotation is defined in its mechanical design. The Rotary Soft Pneumatic Actuator has an inelastic fabric layer which constraints its deflection behavior to a rotational one. This design eliminates the need for an external mechanism to do so, hence reducing its overall footprint.

In summary, both the ideas of generating a specific deflection behavior using the difference in stiffness as well as the idea of defining the center of rotation in the mechanical design are applicable in the development of the eventual soft inflatable rotary actuator. The following section reviews several 3D-printing processes, which are critical to this project.

2.3 3D-Printing Processes

3D-printing is an additive manufacturing process where the material is laid in layers. It is primarily used in rapid prototyping as it is typically fast and a vast selection of materials ranging from plastics to metals and even to composites, can be printed [9]. Each of these materials requires a specific printing process. For this project, two 3D-printing processes were explored: i) Multi Jet Fusion to print HP PA 12 [10] and, ii) Polyjet to print Stratasys Agilus30 [11]. In Multi Jet Fusion, a binding agent is used to fuse the material together when energy is being applied selectively. This fused material eventually becomes the part. For Polyjet, on the other hand, the material is laid one layer at a time. In between each layer, the previous layer is being cured using UV light. With this, the material chosen defines both the printing process and the printer being used. It is worth noting that the mechanical design of a 3D-printed soft inflatable actuator is not entirely free due to the constraints imposed by the printer. The later chapters will cover more on this.

2.4 Design Approach

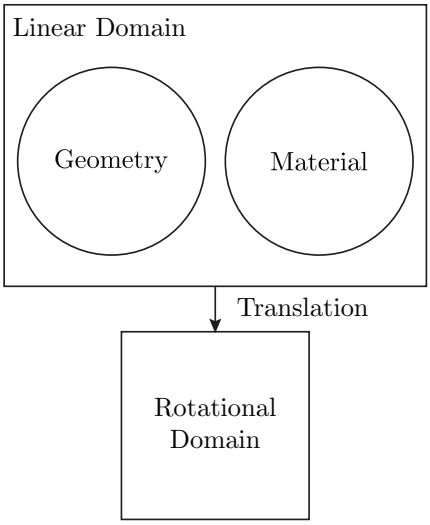

Figure 2.6: Illustration of the adopted design approach.

As mentioned before, the design problem was to develop a 3D-printed inflatable actuator that expands rotationally. The deflection behavior of this soft inflatable actuator has to be designed in a way that it is suitable for a soft robotic arm that has two DoF. Given the limited literature available and the large design space, arbitrarily designing one is very challenging. Hence, one way to circumvent this is to simplify the design problem. The adopted design approach for this project is illustrated in Fig. 2.6. Firstly, instead of exploring all of the possible forms that a soft inflatable actuator can take, this project focused solely on bellow-type ones. This was because bellow-type actuators seemed the most promising, and their underlying mechanics have at least been studied before [12]. Secondly, the design problem was decomposed into two phases, namely the linear domain and the rotational domain. In the linear domain, the effects of geometry and material were studied first. With the insights gained, they were then translated into the rotational domain using a design framework. The underlying assumption made is that these insights will still hold after the translation. Lastly, the insights were used to generate the eventual soft inflatable rotary actuator in the rotational domain. The following chapter explains the first phase of the design process, which is the linear domain.

Chapter 3

Linear Domain

This chapter focusses on the mechanical design of linear bellow-type actuators. The following sections expound upon the two key areas that affect the deflection of these linear actuators, namely its geometry and material.

3.1 Geometry

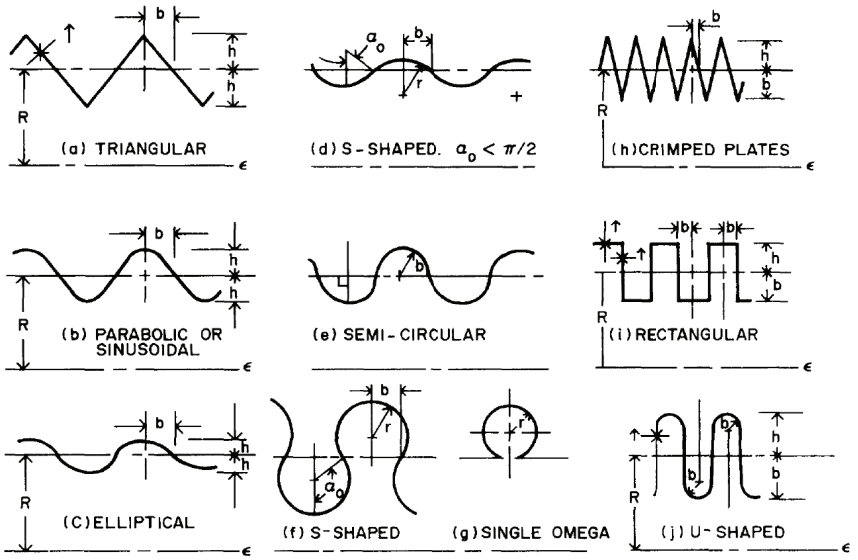

Figure 3.1: Various geometries for linear bellow-type actuators. Reprinted from International Journal of Mechanical Sciences, vol. 26, J.F. Wilson, Mechanics Of Bellows: A Critical Survey, pp. 593 – 603, 1984, with permission from Elsevier. © 1984, Elsevier [12]

Ten possible geometries of a linear bellow-type actuator are introduced in [12] and are shown in Fig. 3.1. Analytical models describing the stiffness of the actuators of different geometries are also introduced. However, the underlying assumption of these models is the idea that the bellow-type actuators are made from hard materials. Hence, these models are not compatible with this project since 3D-printed plastics were the materials of choice. Hence, this project only considered the geometries of these actuators.

It is clear from Fig. 3.1 that the geometries are described by a number of parameters. To better understand what do these parameters refer to, take the actuator as shown in Fig. 3.2 as an example.

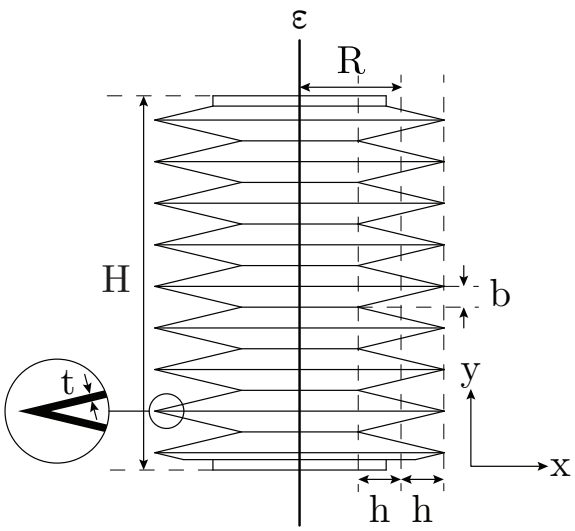

Figure 3.2: Linear bellow-type actuator with Triangular geometry.

Firstly, the geometry revolves around the central axis ϵ, and R denotes the radius from the central axis to the center of the corrugated geometry. Secondly, if the geometry were to be viewed as waves, then h is the X-axis length signifying its amplitude, while b is the Y-axis length representing a quarter of a wavelength. Lastly, H is the Y-axis length denoting the height of the actuator, and t is the wall thickness of the actuator.

From this example, the stated parameters define the geometry in both the X and Y-axis directions. This observation generally holds for other parameterizations such as b, r, and a_0 in the S-Shaped geometry. The b parameter for this case can be calculated using the following equation: $b_s = r\sin(\pi - a_0)$.

It was then desirable to know which out of the ten geometries will enable a linear bellow-type actuator to perform the best. Here, performance is defined as the amount of deflection that the actuator is able to produce for a given internal pressure. Given the number of free design parameters, it made sense to constrain the optimization problem down to a single free parameter and then tune it to obtain maximum deflection. Hence by referring to Fig. 3.2, the following design parameters that describe the various properties of the linear bellow-type actuator were fixed with arbitrary values:

1. $Material$:= HP PA 12: This material was chosen as it can be cheaply and conveniently printed at the Wyss Institute [2].
2. H := 54.0mm
3. R := 12.5mm
4. h := 6.25mm
5. t := 0.500mm: This was chosen near the upper bounds of the capabilities of the printer being used.

In the geometries where the above parameters were not used, these constraints were converted into compatible ones. With these design parameters set, the only free parameter left was b. It was subsequently optimized such that the actuator of that particular geometry obtained the maximum possible deflection when subjected to a given internal pressure. With this, the linear bellow-type actuators of different geometries were first designed in Dassault Systemes SOLIDWORKS. Given

[2]Homepage: http://www.wysszurich.uzh.ch/

that there was no suitable analytical model that described their deflection, FEA was used to estimate it. The in-built FEA tool, SOLIDWORKS SimulationXpress, was used to simulate the Computer-Aided Design (CAD) models with realistic boundary conditions. These are detailed further in Appendices A and B where a linear elastic isotropic model was used in the latter.

3.1.1 Optimization and FEA Results

The steps described in Appendices A and B were repeated manually until a sufficiently good b was found. The relative pressure P_r used in the FEA was chosen to be +1.00 bar. Given the stated constraints, the optimal b parameter of each geometry is listed in Table 3.1.

Geometries	b [mm]	Normalized Deflection δ_n
Crimped Plates	1.00	0.431
Triangular	1.50	0.346
Elliptical	1.50	0.982
Rectangular	2.50	0.555
S-Shaped	2.80	0.357
U-Shaped	1.00	2.46

Table 3.1: Optimal b parameters for the various geometries. The deflection of the linear bellow-type actuators have been normalized over its initial heights $H = 54.0$mm.

Out of the ten geometries introduced in [12], four were neglected. They were the S-Shaped ($a_0 < \pi/2$), Semi-Circular, Parabolic or Sinusoidal and Single Omega geometries. When designing the first two using the constraints given, it was clear to see that they both have a form which will perform poorly. For the Parabolic or Sinusoidal geometry, the CAD model generated was unable to be meshed for FEA, regardless of what mesh parameters were being used. This may be due to the continuously differentiable nature of the geometry which made it difficult for it to be decomposed into triangles needed for FEA. For the Single Omega geometry, it simply did not make any physical sense.

From Table 3.1, the U-Shaped geometry was predicted to perform the best. The FEA results also seem to suggest that the total internal surface area of these linear bellow-type actuators is proportional to its deflection. In other words, the larger the internal surface area, the more compliant the part will be.

In the following subsection, the linear bellow-type actuators were 3D-printed and physically experimented.

3.1.2 Physical Experimentation

The generated CAD files were printed using HP PA 12 at the Wyss Institute. The 3D-printed parts are as shown in Fig. 3.3. Due to the printing process (Multi Jet Fusion), the parts have a powdery texture to them and required cleaning. Once cleaned, the flange and air supply tube were subsequently glued to the parts using adhesives (Loctite 406 and Loctite SF 770). They were then left to cure for a day. After this, they were pressure tested.

The linear bellow-type actuators were each placed in a blast-resistant enclosure and subjected to relative pressures from 0.00 bar to +1.80 bar in steps of +0.20 bar using a compressor. The internal pressures of the parts, as well as their linear deflection, were recorded. The pressures were recorded using a Bürkert 8230 pressure sensor while, the linear deflection was derived from the recorded test footage.

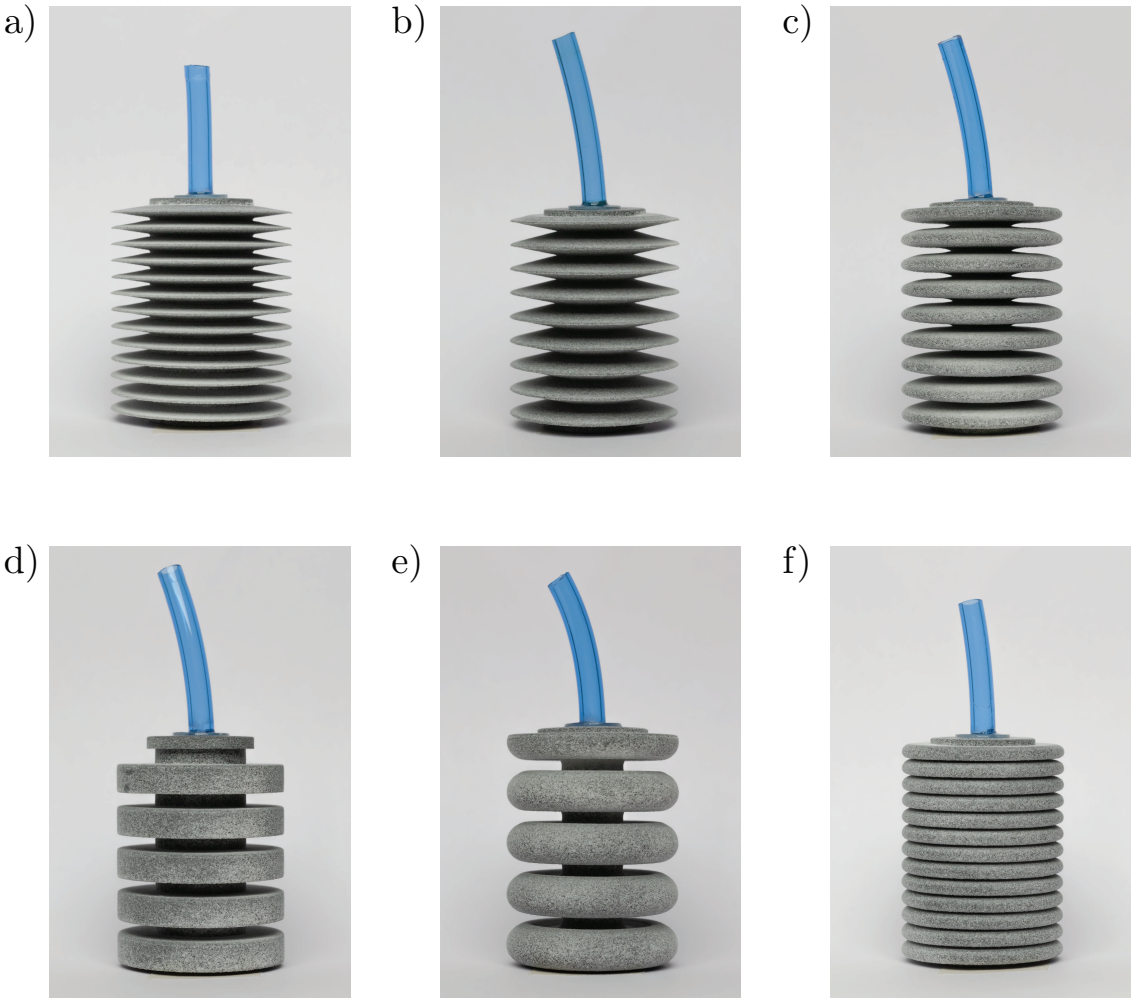

Figure 3.3: The 3D-printed linear bellow-type actuators of different geometries. a) Crimped Plates geometry. b) Triangular geometry. c) Elliptical geometry. d) Rectangular geometry. e) S-Shaped geometry. f) U-Shaped geometry.

The results from the conducted experiment and their respective FEA predictions were used to generate Figs. 3.4 and 3.5 are shown below.

Focusing on the difference between the actual experimental data and the FEA predictions, the plots in Fig. 3.4 convey three key insights. Firstly, the FEA tool being used, SOLIDWORKS SimulationXpress treated the parts as linear springs as seen from the linear blue lines. This was not the case in reality as seen from the red lines each tending towards a horizontal asymptote. Secondly, the FEA predictions were inconsistent. It was able to predict rather accurately for half of them and not so for the other half. Last but not least, the FEA predictions tended to overestimate the deflection of these parts. One possible reason behind these deviations could be that the elastic model used by the FEA tool was inadequate in accounting for the plastic deformation of the parts. This may be solved by using the full-fledged version of the FEA tool, SOLIDWORKS Simulation where multiple elastic models can be chosen.

Figure 3.5 shows all of the experimental data in a single plot. It is clear that the U-Shaped geometry was the best performing one in terms of normalized deflection per relative pressure, as compared to the other geometries. This result was in accordance with the FEA predictions, as shown in Table 3.1. Hence, this highlights the value that FEA has in such design problems.

To summarize, this section examines the effect of geometry on the deflection of linear bellow type actuators. It was found that given the design constraints, the U-Shaped geometry was the optimal one. Hence, it should be integrated into the mechanical design of the eventual soft inflatable rotary actuator. The material effects on the deflection of this type of actuator are explored in the next section.

3.2 Material

This section explores the effects of using Stratasys Agilus30 as the material for the linear bellow-type actuators

Stratasys Agilus30 is a rubber-like material that is designed to be both flexible and tear-resistant. This material was chosen as it was interesting to know the effects that such a flexible plastic has on the deflection behavior of linear bellow-type actuators, as compared to a more typical plastic such as HP PA 12.

To understand the material better, the steps described in Appendices A, B and Subsection 3.1.1 were being carried out. However, some changes were made to the part. The wall thickness and initial height were changed to $t = 1.50$mm and $H = 56.0$mm. The former was recommended by the 3D-printing company, alphacam [3] which was responsible for printing the parts. With that, the table below presents the FEA results:

Geometries	b [mm]	Normalized Deflection δ_n
Crimped Plates	3.00	$1.37*10^3$
Triangular	2.00	$2.73*10^3$
Elliptical	3.50	$3.02*10^3$
Rectangular	3.75	$3.64*10^3$
S-Shaped	2.86	$5.75*10^3$
U-Shaped	1.75	$4.94*10^3$

Table 3.2: Optimal b parameters for the various geometries. The deflection of the linear bellow-type actuators have been normalized over its initial heights $H = 56.0$mm.

From Table 3.2, two things were observed. Firstly, the normalized deflection of the models were significantly greater than those shown in Table 3.1. This was due to the compliant nature of Stratasys Agilus30 being embedded into its material profile as well as the same relative pressure being used in FEA ($P_r = +1.00$ bar). Additionally, it was observed that given the new design constraints, FEA predicted that the S-Shaped geometry will perform the best. This was likely due to the increased wall thickness and its relations to the other design constraints. With this insight, two linear bellow-type actuators with the S-shape geometry and different wall thicknesses ($t = \{1.50, 3.00\}$mm) were being printed using Stratasys Agilus30 by alphacam. This was done to investigate the effects of differing wall thicknesses as well. The parts are as shown in Fig. 3.6. As a side note, only these two parts were printed due to the high costs involved with printing and post-processing (cleaning the supporting structures with chemicals).

Like their HP PA 12 counterparts, the Stratasys Agilus30 parts were first cleaned after printing and then glued with the necessary flange and air supply tube. They were then left to cure for a day. After curing, these parts were subjected to pressure testing. Since the parts were very flexible, they did not require the use of the compressor and were hand-pumped using a syringe instead. The deflections of these parts were measured using a ruler while the mentioned pressure sensor measured the internal pressures of these parts. The plot of the recorded experimental data is as shown in Fig.

[3] Homepage: https://www.alphacam.ch/

3.7. While FEA was also being carried out using the experimental conditions, the predictions were inaccurate (unrealistic amounts of deflection predicted). Hence, it was not included in Fig. 3.7, and it highlights the difficulty when predicting the deflection behavior of such flexible materials.

Two insights can be gained from Fig. 3.7. Firstly, it can be seen that the parts printed using Stratasys Agilus30 were able to deflect greatly at very low pressures ($\delta_n \approx 1.60$ at $P_r \approx +0.17$ bar) which is greater than the U-Shaped HP PA 12 part at significantly higher pressures ($\delta_n \approx 1.40$ at $P_r \approx +1.80$ bar). Secondly, the wall thicknesses of the parts seem to be unimportant in determining the deflection behavior of the parts. However, in terms of robustness, a part with thicker walls will be more resistant to physical damage.

In summary, the flexible material, Stratasys Agilus30 was shown to be a promising 3D-printing material for the eventual soft inflatable rotary actuator as it enables the fulfillment of the design requirement of actuating using low pressures.

A design framework that translates the insights into the rotational domain will be introduced in the following chapter. Additionally, the mechanical design of the eventual soft inflatable rotary actuator is also presented.

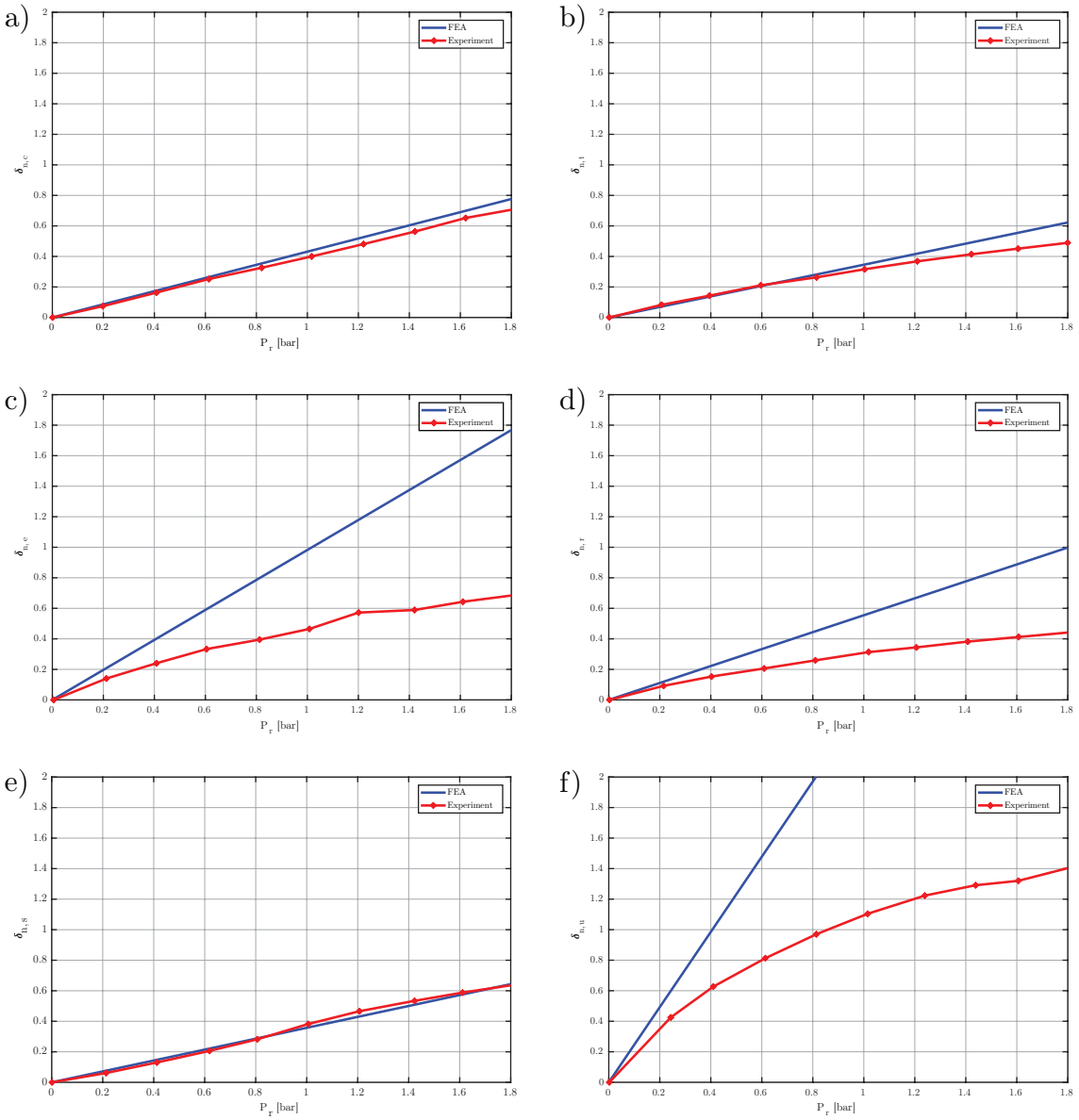

Figure 3.4: FEA predictions and experimental data plots of the printed actuators. The X-axis represents the relative pressures that the parts were subjected to P_r. The Y-axis represents the normalized deflection of the parts over their initial lengths δ_n. The blue line represents the FEA data. The red line represents the experimental data. a) Crimped Plates geometry. b) Triangular geometry. c) Elliptical geometry. d) Rectangular geometry. e) S-Shaped geometry. f) U-Shaped geometry.

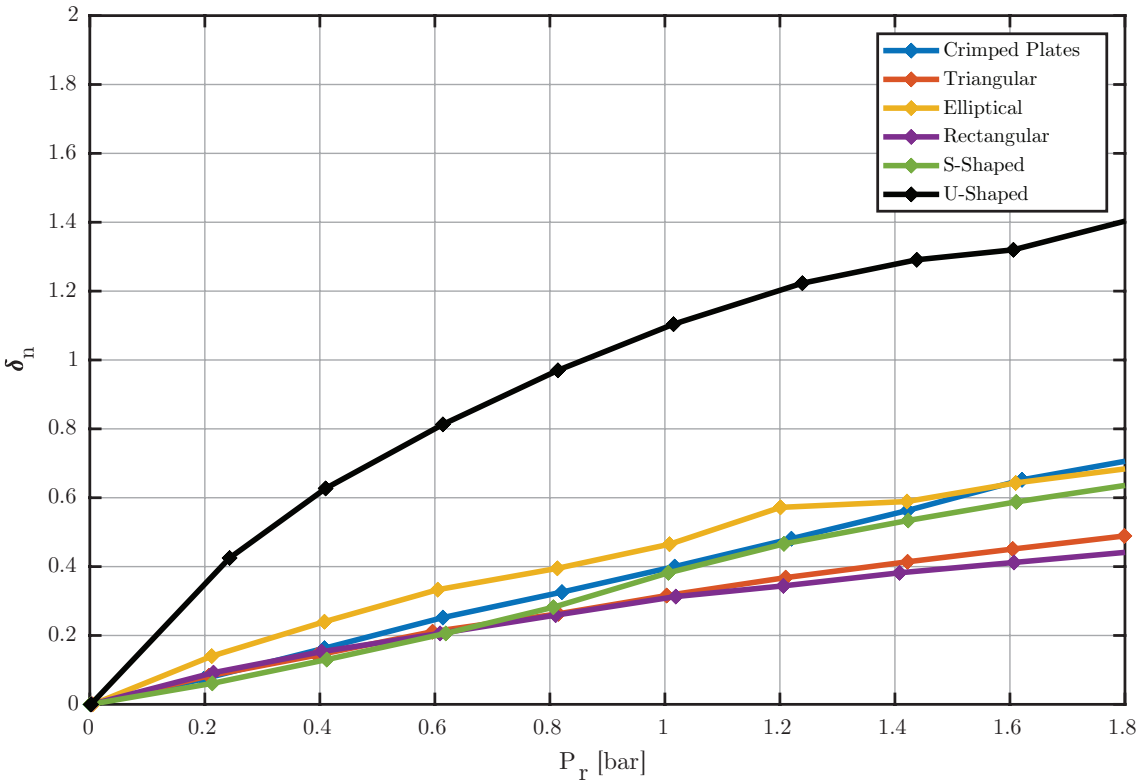

Figure 3.5: Experimental data showing the deflection behaviors of the different geometries. The X-axis represents the relative pressures that the parts were subjected to P_r. The Y-axis represents the normalized deflection of the parts over their initial lengths δ_n. The deflection behaviors of the Crimped Plates, Triangular, Elliptical, Rectangular, S-Shaped, and U-Shaped geometries are represented by the blue, red, yellow, purple, green and black lines respectively.

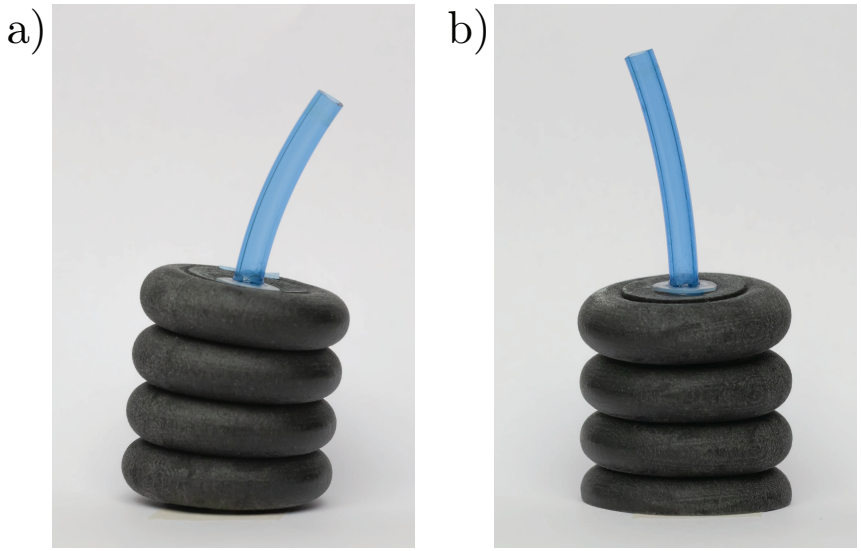

Figure 3.6: The 3D-printed linear bellow-type actuators using Stratasys Agilus30. a) S-Shaped geometry with $t = 1.50$mm. b) S-Shaped geometry with $t = 3.00$mm.

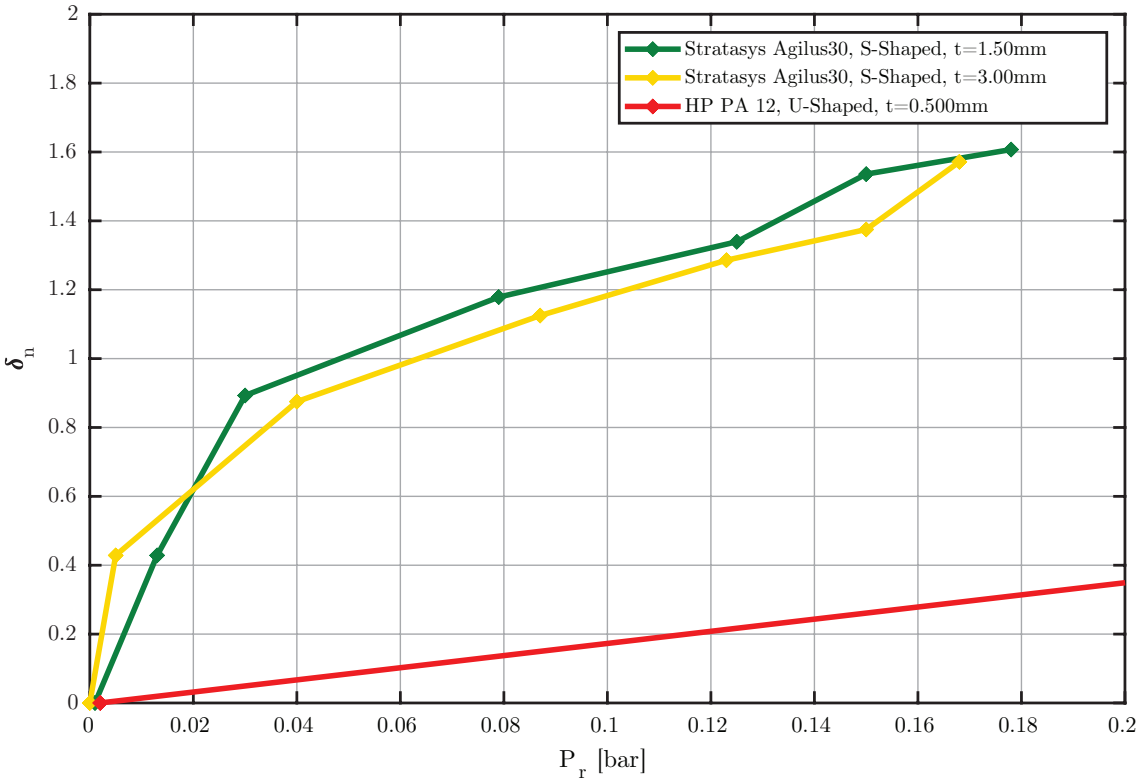

Figure 3.7: Experimental data showing the deflection behaviors of the parts printed with Stratasys Agilus30 and the U-Shaped one with HP PA 12 for comparison. The X-axis represents the relative pressures that the parts were subjected to P_r. The Y-axis represents the normalized deflection of the parts over their initial lengths δ_n. The deflection behaviors of the parts printed with Stratasys Agilus30 and having wall thicknesses $t = \{1.50, 3.00\}$mm are represented by the green and yellow lines respectively. The deflection behavior of the part printed with HP PA 12 and having the U-Shaped geometry, and a wall thickness $t = 0.500$mm is represented by the red line.

Chapter 4

Rotational Domain

This chapter expounds on how the insights gained were being translated from the linear domain into the rotational domain. These were then utilized to develop the eventual soft inflatable rotary actuator. The underlying assumption being that the insights will still hold after translation.

4.1 Translation Design Framework

After obtaining the insights, a question that naturally arose was on how they can be used to develop the mechanical design of the soft inflatable rotary actuator. This question arose because there was no literature available to hint on the form of a soft inflatable rotary actuator that is capable of enabling a two rotational DoF motion. After much thinking, the design problem was solved using fundamentals. This is the key idea behind the translation design framework being developed and used, which will be explained in the next paragraphs.

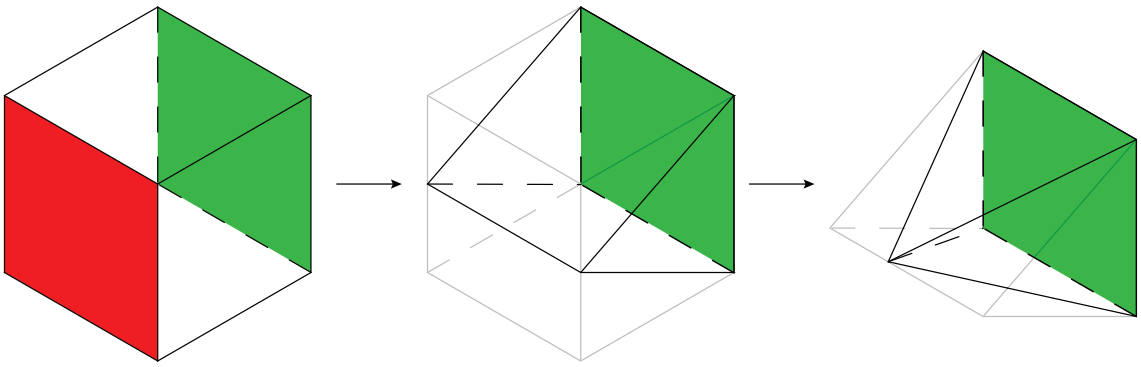

Figure 4.1: Design framework being used to translate the insights from the linear domain to the rotational domain. The color green signifies the face which has to be the most compliant, while the color red signifies the face which has to be the least compliant or in other words, most stiff.

The figure above illustrates the translation design framework and serves as a visual aid in the understanding of the concept. This design framework begins by focusing on the form of a soft inflatable actuator. The simplest form that one can be reduced to is a cube. Simplest here means that there is no assumption on the deflection behavior of the soft inflatable actuator. In order to create a rotary actuator (one rotational DoF motion), the insights regarding asymmetry and defining the center of rotation were implemented. The furthest face is arbitrarily chosen as the face where deflection has to be the most pronounced (in green). In other words, this face has to be the most compliant. One way is to increase its internal surface area as much as possible, say

by implementing a particular bellow geometry here. Next, the center of rotation is defined. The opposite face can be assigned as the pivot (in red) and should be as stiff as possible, preferably rigid. This face is certainly rigid if it is reduced into a single line. This face has essentially been transformed into an axis of rotation. With this, the proper form of a soft inflatable rotary actuator for a one rotational DoF motion is obtained. This form is the same form that is seen in the current iteration of the soft robotic arm as shown in Fig. 2.1, as well as the Rotary Soft Pneumatic Actuator [8] as shown in Fig. 2.5. Using intuition, for a two rotational DoF motion, this axis of rotation needs to be further reduced into a single point where all of the actuators actuate about (point of rotation). With that, the proper form of a soft inflatable rotary actuator for a two rotational DoF motion is in the form of a pyramid.

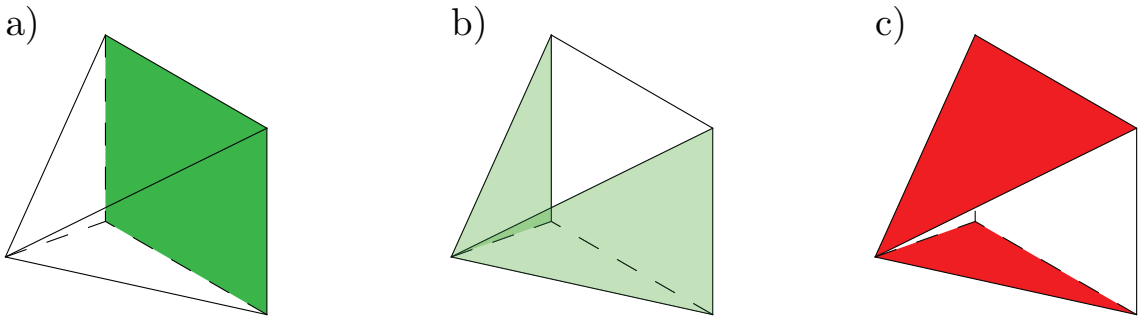

Figure 4.2: Assigning stiffnesses to the various faces of the soft inflatable rotary actuator. The color green signifies the face which has to be made the most compliant, while the color red signifies the face which has to be made as stiff as possible. a) The furthest face where deflection has been chosen to be the greatest. b) The side faces where they have to be compliant enough to facilitate the desired deflection on the primary face. c) Top and bottom faces where they have to be made as stiff as possible.

Another question that subsequently arose was regarding the stiffness of the other faces. The linear models did not cover the boundary conditions of the mechanical design since they are symmetrical about their central axis. Fortunately, using intuition again, it suggests that the sides have to be compliant enough to facilitate the deflection on the primary face of the pyramid. Additionally, the top and bottom faces have to be made as stiff as possible to ensure the deflection behavior is contained and that the soft inflatable rotary actuator expands about its point of rotation. This is similar to the one used in the Soft Pneumatic Actuator [8] where an inextensible material was used to contain the deflection behavior. These points are illustrated in Fig. 4.2 above. With these issues settled, the actual mechanical design of the soft inflatable rotary actuator was finally started.

4.2 FEA Predictions and Physical Experimentation

The CAD files of a soft inflatable rotary actuator with flat sides and another with lofted sides were generated using the steps described in Appendices C and D. It is worth noting that the design parameters used in these designs were not optimal as the design process was constrained by the tools used in SOLIDWORKS (especially for the one with loft sides). The models were put through FEA (following the steps as described by Appendix B) with a relative pressure of +1.00 bar. The FEA predictions on its deflection behavior are shown in Table 4.1 and Fig. 4.3 below.

The FEA predictions were assessed in two ways, namely the amount of deflection for the given pressure and the qualitative deflection behavior (animation). It was found through the various iterations that the deflection behavior of the parts was sensitive to the parameters used to describe the U-Shaped geometry. For example, if extreme values of the parameters were used such that it resulted in deep folds, the folds would wobble and eventually not give rise to the desired deflection behavior. Hence the need for the two-pronged assessment.

Sides	Angular Deflection θ [°]
Flat	24.1
Lofted	97.3

Table 4.1: FEA predictions on the angular deflections of the parts with different sides. The FEA predictions were initially in [mm], they were then converted into [°] using the following equation: $\theta = (180/\pi)(\delta/R)$ where δ is the FEA prediction in [mm] and R is the radius from the point of rotation to the center of the corrugated geometry used.

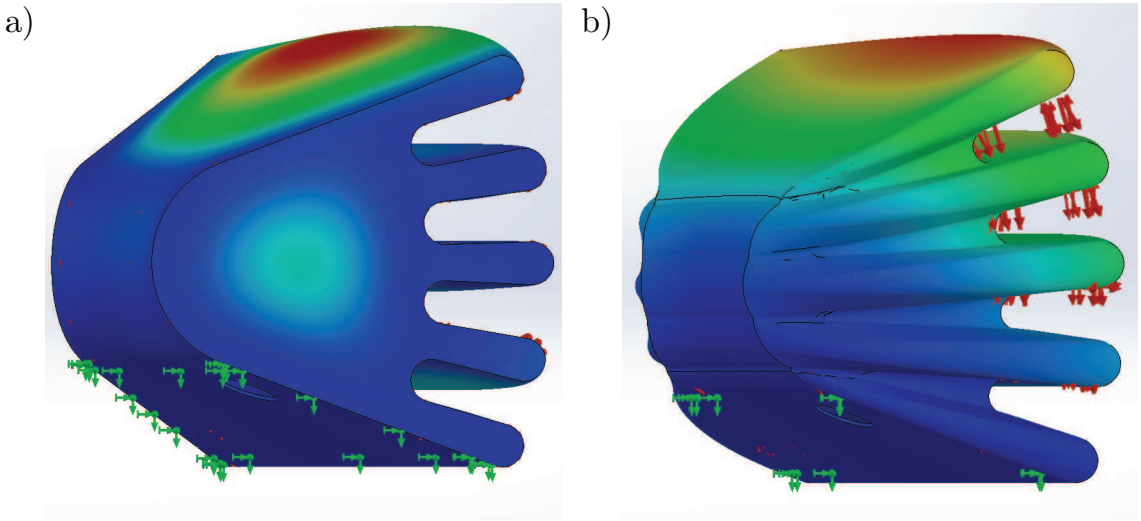

Figure 4.3: Predicted FEA deflection behavior. The deflections have been normalized using a color scale that runs from red to blue. The color red signifies the areas where deflection is the greatest. The color blue signifies the areas where deflection is lowest. a) Flat sides. b) Lofted sides.

The FEA predictions convey two key findings. Firstly, in terms of the amount of deflection, the one with the lofted sides emitted a higher angular deflection than the one with flat sides. Secondly, by looking at both the predicted deflection behavior animations as well as the deflection distributions, the one with lofted sides deflected rotationally with a more gradual deflection distribution. This suggests that the one with the lofted sides was performing just as desired. On the other hand, the one with flat sides has an unusual deflection behavior. It has undesired deflections on its sides as well as on its folds, suggesting that it was inferior to the one with a lofted side. Overall, these findings validate not only the mechanical designs of the soft inflatable rotary actuators but also the translation design framework that was detailed in Section 4.1.

The parts were printed in HP PA 12, as shown in Fig. 4.4. As a side note, the parts were not printed in Stratasys Agilus30 due to the high costs involved and the uncertainty in the actual behavior of these parts.

Like the other parts before, the printed parts were cleaned and had their flange and air supply tube glued. Once cured, the parts were subjected to pressure testing with relative pressures from 0.00 bar to +1.00 bar in 0.20 bar steps using the same setup as mentioned in Subsection 3.1.2. Figs.4.5 and 4.6 respectively show the deflection behavior of the parts during the experiment as well as the results.

The experimental results convey the following insights. Firstly, the qualitative description of the deflection of the parts by FEA is accurate. From Fig. 4.5, it can be seen that the one with lofted sides expanded in a consistent rotational manner just as predicted, while the one with the flat

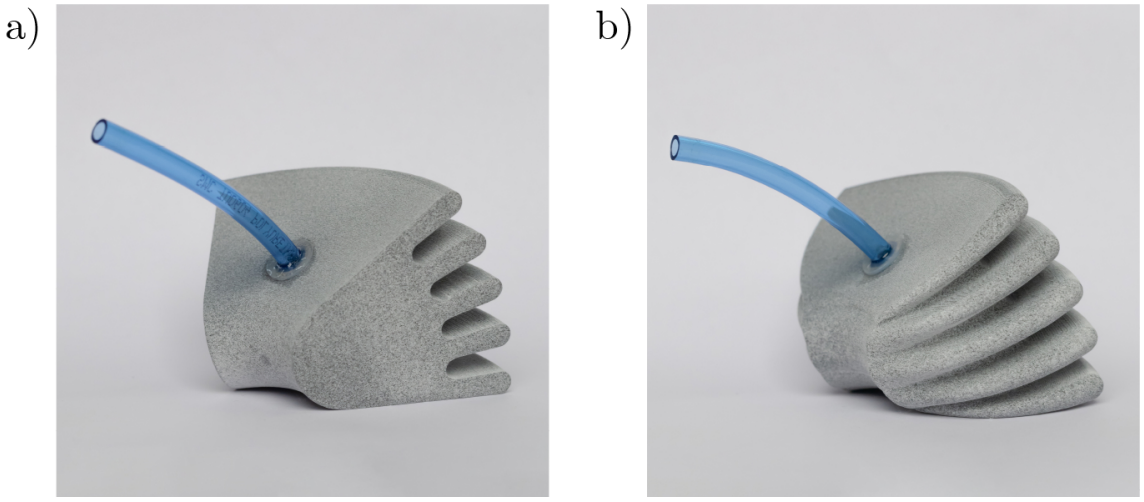

Figure 4.4: The 3D-printed inflatable rotary actuators using HP PA 12. a) Flat sides. b) Lofted sides.

sides underwent some irregular plastic deformation on its top, sides, and bottom. Secondly, with regards to the actual deflection predictions, FEA is only able to predict accurately if the part had a regular deflection behavior. This is seen from the small deviations that the FEA predictions have with the actual data of the one with lofted sides. Comparing this with the one with flat sides, there are large deviations between the FEA and actual experimental data as FEA was unable to account for the unusual plastic deformations of the part. Last but certainly not least, the data physically validates the translation design framework that was detailed in Section 4.1.

All in all, these results strongly substantiate the mechanical design of the 3D-printed inflatable rotary actuator with lofted sides as the first conceptual prototype for the soft robotic arm with two DoF as all of the design requirements formulated in Section 2.1 have been adequately fulfilled.

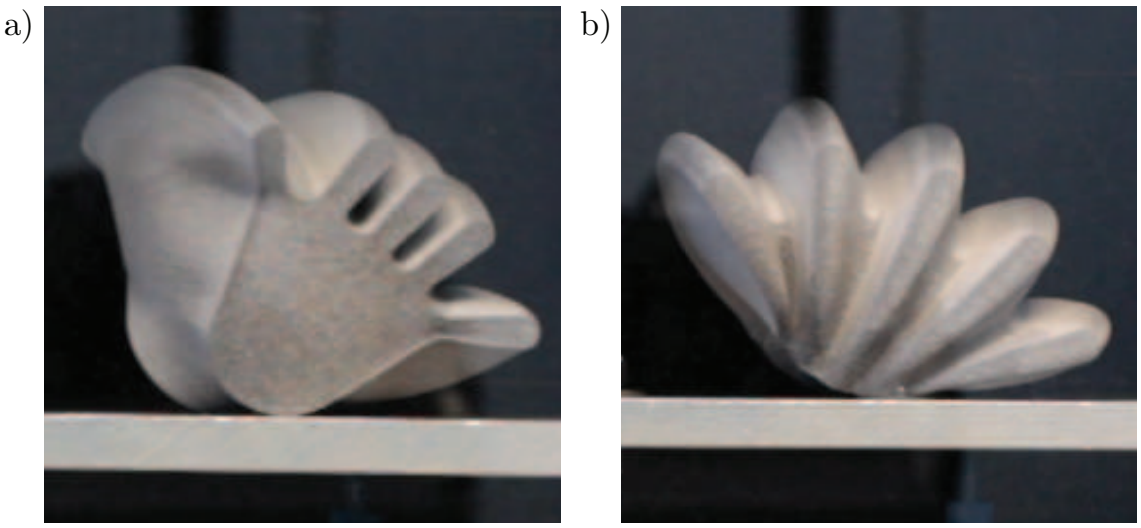

Figure 4.5: The soft inflatable rotary actuators at maximum deflection during the conducted experiments. a) Flat sides. b) Lofted sides.

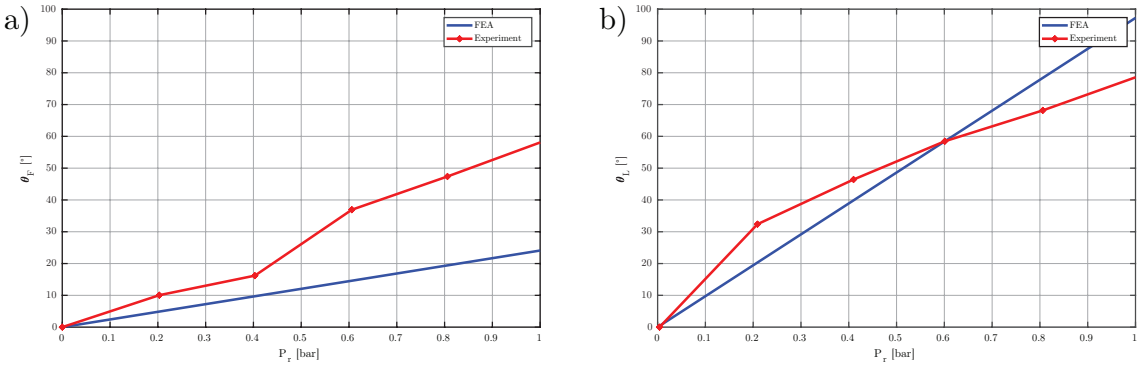

Figure 4.6: Experimental data showing the deflection behavior of the different sides. The X-axis represents the relative pressures that the parts were subjected to. The Y-axis represents the absolute angular deflection of the parts. a) Flat sides. b) Lofted sides.

Chapter 5

Conclusion

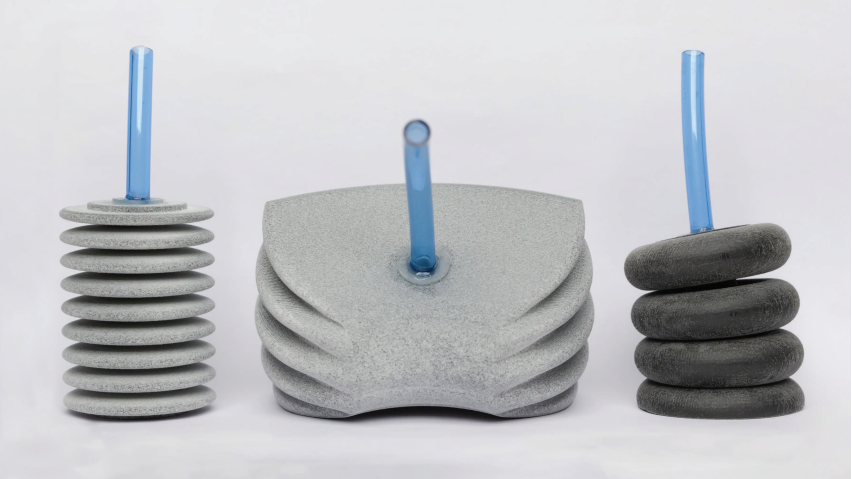

Figure 5.1: The different types of 3D-printed inflatable actuators explored.

This semester project explored the mechanical design of 3D-printed inflatable actuators, where it sought to develop a 3D-printed inflatable rotary actuator for a soft robotic arm with two 2 DoF. The design problem was first simplified into two phases due to its complexity. In the first phase, linear actuators were developed, and the effects of geometry and material were studied. These insights were then translated in a second phase to the rotary domain. In the second phase, the insights were utilized to generate the mechanical design of the eventual soft inflatable rotary actuator. Through simulation and physical experimentation, it was shown to emit high angular deflection at relatively low pressures. In conclusion, the realized 3D-printed inflatable rotary actuator is an effective first conceptual prototype for the future soft robotic arm with two DoF.

Future work involves the following:

1. Further exploring the use of flexible materials and their application in the rotational domain (e.g. fatigue behavior).
2. Integrating all of the mentioned insights and jointly optimizing the design parameters.
3. Exploring 3D-printing for the other structural components of the soft robotic arm. The aim is to reduce the overall weight and inertia of the soft robotic arm.

With the above, it is hoped that the envisioned arm, as shown in Fig. 5.2 can be realized.

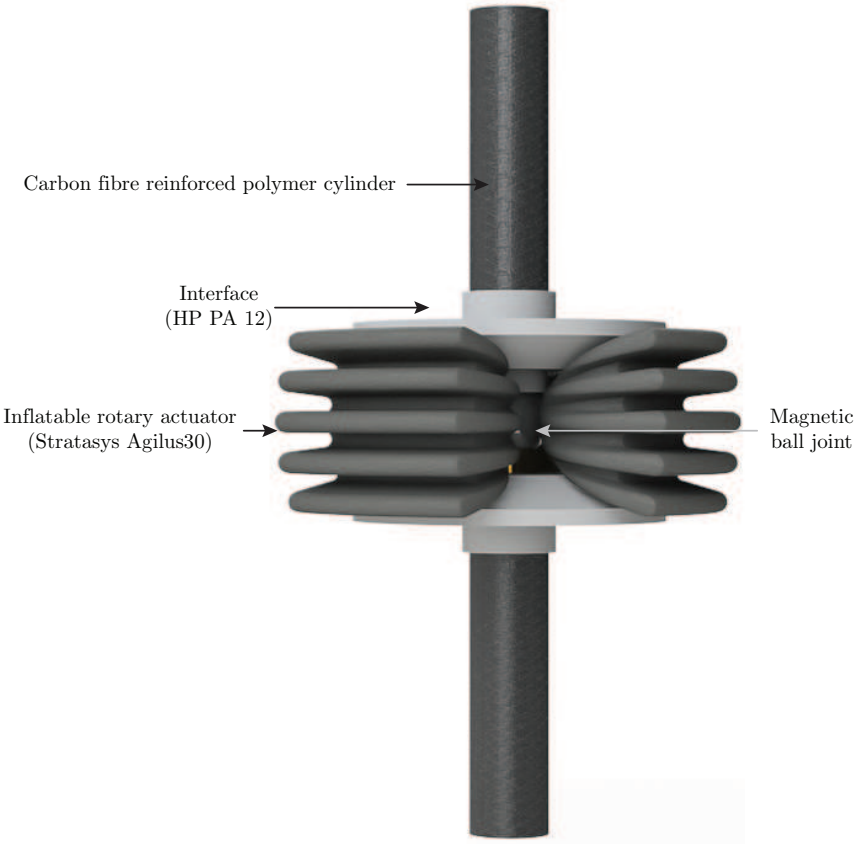

Figure 5.2: Rendering of the envisioned pneumatically-actuated soft robotic arm with two DoF.

Appendix A

Designing a Linear Bellow-type Actuator in SOLIDWORKS

This appendix is a walk-through describing how the CAD model of a linear bellow-type actuator can be created in SOLIDWORKS. The actuator will be designed using a bottom-up approach since pressurized air is injected from the bottom. The dimensions stated in this walk-through are the ones used for this project. If different components are used, these dimensions have to be changed accordingly. The following are the steps describing the CAD process:

1. Open SOLIDWORKS and create a new part file.
2. Select the top plane and start a new sketch.
3. Draw a circle with a diameter of 25.0mm. This will be the base of the actuator.
4. At the center of this circle, draw another circle with a diameter of 8.50mm. This is a hole meant for a flange where the air supply tube will be connected to.
5. Exit the sketch and extrude it by 2.00mm using the Extrude Boss/Base tool.
6. Now select the front plane and start another sketch. Draw the desired geometry here.
7. Exit the sketch. With the geometry now properly defined, an infinitesimally thin surface of the geometry can now be created (Insert > Surface > Revolve).
8. This surface is then thickened to the desired value of 0.500mm (Insert > Boss/Base > Thicken). This way of defining the thickness of the walls is simpler and more efficient than defining it in a sketch. This is because the thickness is now a parameter that can be easily changed. However should the surface be unable to thicken, it means either of two things. The thickened surfaces could either be intersecting one another or are too close to one another. Make the necessary changes depending on the situation.
9. Now the end cap of the actuator can be designed. Repeat Steps 2, 3, and 5 at the desired height of 50.0mm away from the base.
10. Combine the pieces by selecting the bodies in the Solid Bodies option on the left pane and combine them.

With these steps, the CAD model of the linear bellow-type actuator is obtained.

Appendix B

Performing FEA using SOLIDWORKS SimulationXpress

This appendix is a walk-through describing the procedure of performing an FEA on an inflatable actuator of interest. The FEA tool used is SOLIDWORKS SimulationXpress. While it is a simplified version of the full-fledged tool SOLIDWORKS Simulation, its features are sufficient enough to get some first insights about the mechanical design.

Material Properties	Values
Elastic Modulus [N/m^2]	$1.70*10^9$
Poisson's Ratio	$4.00*10^{-1}$
Mass Density [kg/m^3]	$1.01*10^3$
Tensile Strength [kg/m^3]	$4.80*10^{10}$

Table B.1: Material properties of HP PA 12

Material Properties	Values
Elastic Modulus [N/m^2]	$1.00*10^5$
Poisson's Ratio	$4.50*10^{-1}$
Mass Density [kg/m^3]	$9.60*10^2$
Tensile Strength [kg/m^3]	$2.40*10^6$

Table B.2: Material properties of Stratasys Agilus30

Before proceeding any further, Tables B.1 and B.2 show the generated SOLIDWORKS material profiles for HP PA 12 and Stratasys Agilus30 respectively. These material profiles were used in the FEA. The key properties regarding HP PA 12 were from [10]. However, its Poisson's Ratio is estimated from similar plastics. For Stratasys Agilus30, on the other hand, only its tensile strength was derived from [11]. The other properties were estimated from rubber. With that, the following are the steps describing the FEA process:

1. Open the SOLIDWORKS part file containing the actuator of interest.
2. Start SOLIDWORKS SimulationXpress (Evaluate > SimulationXpress Analysis Wizard)

3. Start a new study.
4. Select the bottom face of the base plate as the fixture.
5. View the cross-section of the actuator (Section View, Front Plane).
6. Subject the internal surfaces of the actuator to the desired pressure. Ensure that all internal surfaces are selected and note the direction of the applied pressure.
7. Choose the desired material profile.
8. Select an appropriate mesh density. It is recommended to choose Mesh Parameters of 1.00mm and 0.05mm. While it may take a relatively long time to process the part, it is applicable to most geometries.
9. Mesh the part and run the simulation.
10. Observe the deflection animation. A linear actuator should deflect in the vertical Y-axis direction, while a rotary actuator should deflect rotationally.
11. Record the predicted deflection value. Otherwise, an FEA report may also be generated if desired.

With these steps, FEA has been performed on the actuator of interest.

Appendix C

Designing a Soft Inflatable Rotary Actuator with Flat Sides in SOLIDWORKS

From Section 4.1, it was known that the sides of the soft inflatable rotary actuator have to be made compliant in order to facilitate its deflection on the primary face. As such, two mechanical designs of the sides were explored, namely, the flat sides and the lofted sides.

As their name suggests, the flat sides are essentially thin walls. They are relatively simple to create in SOLIDWORKS, and this design serves as a baseline for comparison. For this example, it is assumed that the part will be printed in HP PA 12. Hence the bellow geometry of choice is the U-Shaped one. In the following, the procedure to generate the CAD of a soft inflatable rotary actuator with flat sides is described:

1. Open SOLIDWORKS and create a new part file.
2. Select the top plane and create a new sketch.
3. Sketch the following guides: i) An infinite vertical line that intersects with the origin. ii) An infinite horizontal line that intersects with the origin. iii) Three circles to guide the U-Shaped geometry. For this example, the following diameters were used $D = \{138, 150, 162\}$mm. These diameters indicate that a modified U-shaped geometry is being used. Using the wave analogy for the sake of simplicity, $h = 12.0$mm is used to define both the positive and negative amplitudes (note that this is different from the original U-shaped geometry as shown in Fig. 3.1, where b is used to define the negative amplitude).
4. Follow the sketch, as shown in Fig. C.1. Do note that $b = 3.00$mm, the guidelines intersect the origin as well as are tangent to the circles and that the lines which connect the circles are collinear with the guidelines. The number of folds drawn was arbitrarily chosen to keep the size of the actuator small.
5. By using the Trim Entities tool, delete the lines that are not needed as shown in Fig. C.2.
6. By using the Mirror Entities tool, reflect the sketch about the horizontal line and fillet the lines which intersect at the origin. A fillet of 15.0mm was also arbitrarily chosen. The sketch, as shown in Fig. C.3 should be obtained.
7. With the geometry now properly defined, an infinitesimally thin surface of the geometry can now be created (Insert > Surface > Revolve). Revolve to the desired angle, it is 60.0° for this case. Knit the surfaces together (Insert > Surface > Knit) to form a single surface.

8. This surface is then thickened to the desired value of 0.50mm (Insert > Boss/Base > Thicken). However should the surface be unable to thicken, it means either of two things. The thickened surfaces could either be intersecting one another or are too close to one another. Make the necessary changes depending on the situation. The part, as shown in Fig. C.4 should be obtained.
9. Select the face of one side and create a sketch there. While selecting that face, use the Convert Entities tool to obtain the outline of that side.
10. Extrude it by 0.500mm to get the flat side.
11. Repeat Step 9 and 10 for the other side.
12. Create a plane (Insert > Reference Geometry > Plane). Select the front plane as the reference and offset it by 30.0mm.
13. Select the plane and follow the sketch, as shown in Fig. C.5. The circle here is used to cut the hole for the flange.
14. Using the Extrude Cut tool, cut the hole into the bottom side of the part.

With these steps, the CAD model of the soft inflatable rotary actuator with flat sides is completed, as shown in Fig. C.6.

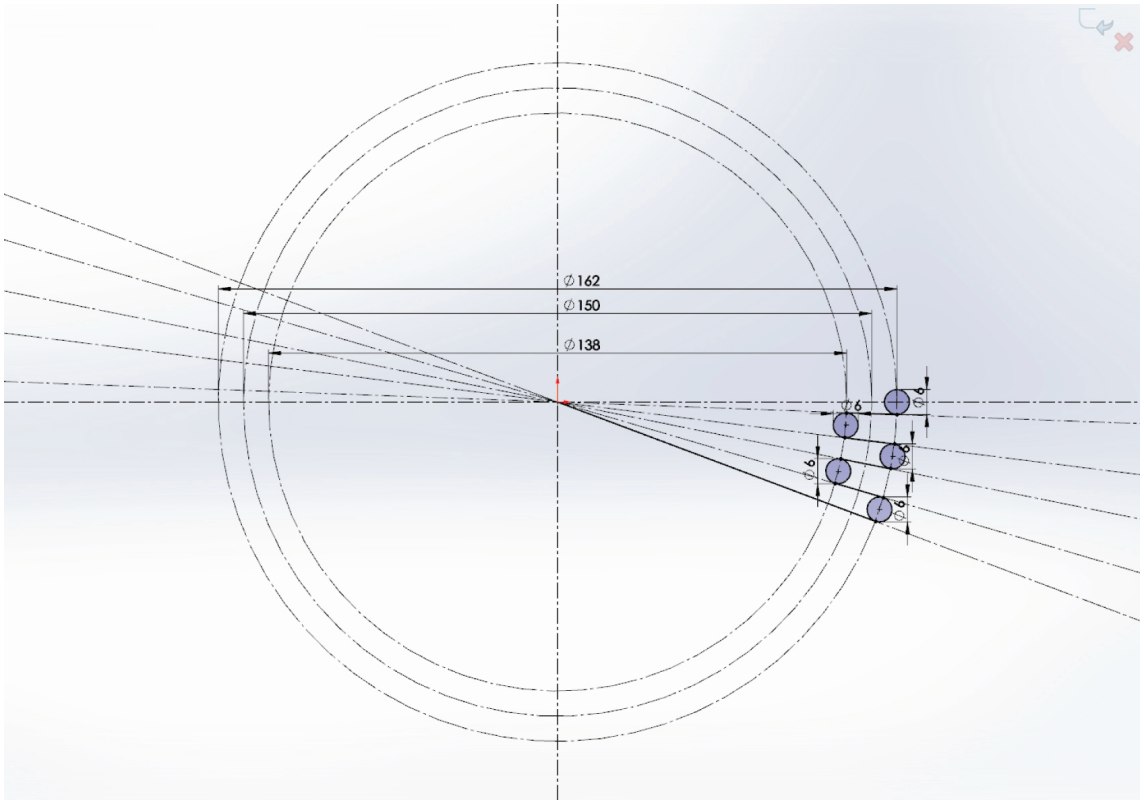

Figure C.1: Step 4.

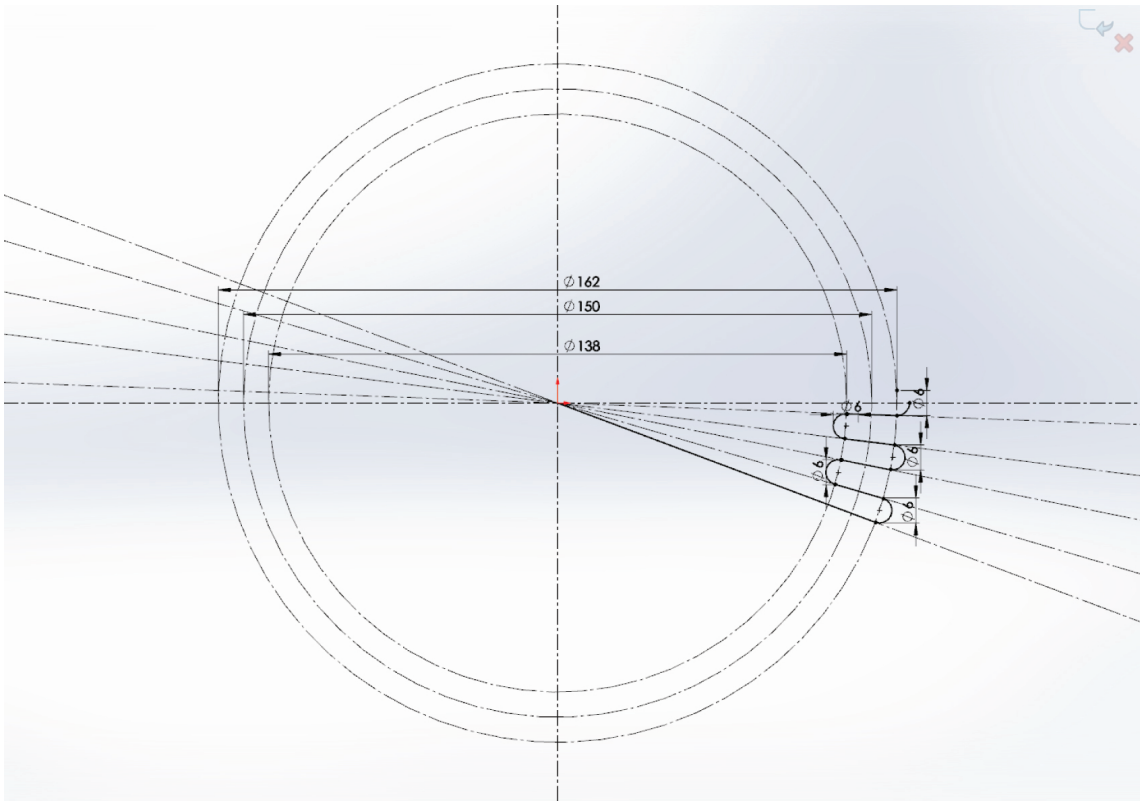

Figure C.2: Step 5.

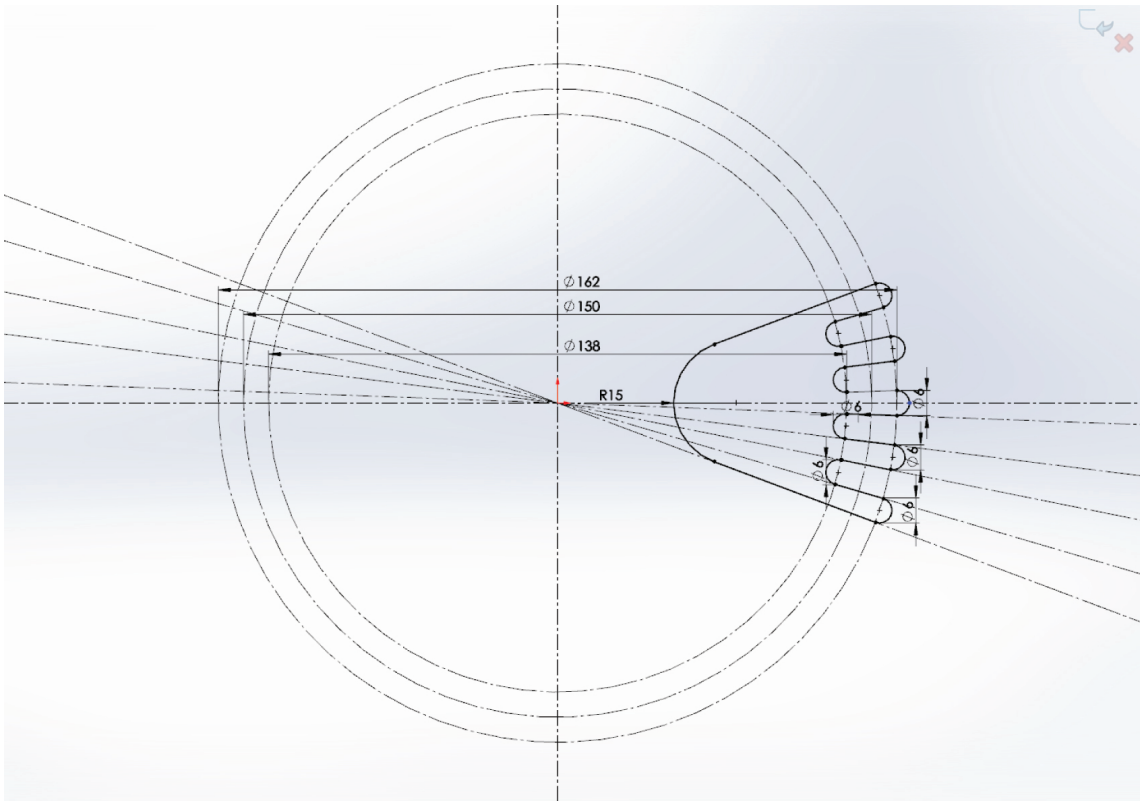

Figure C.3: Step 6.

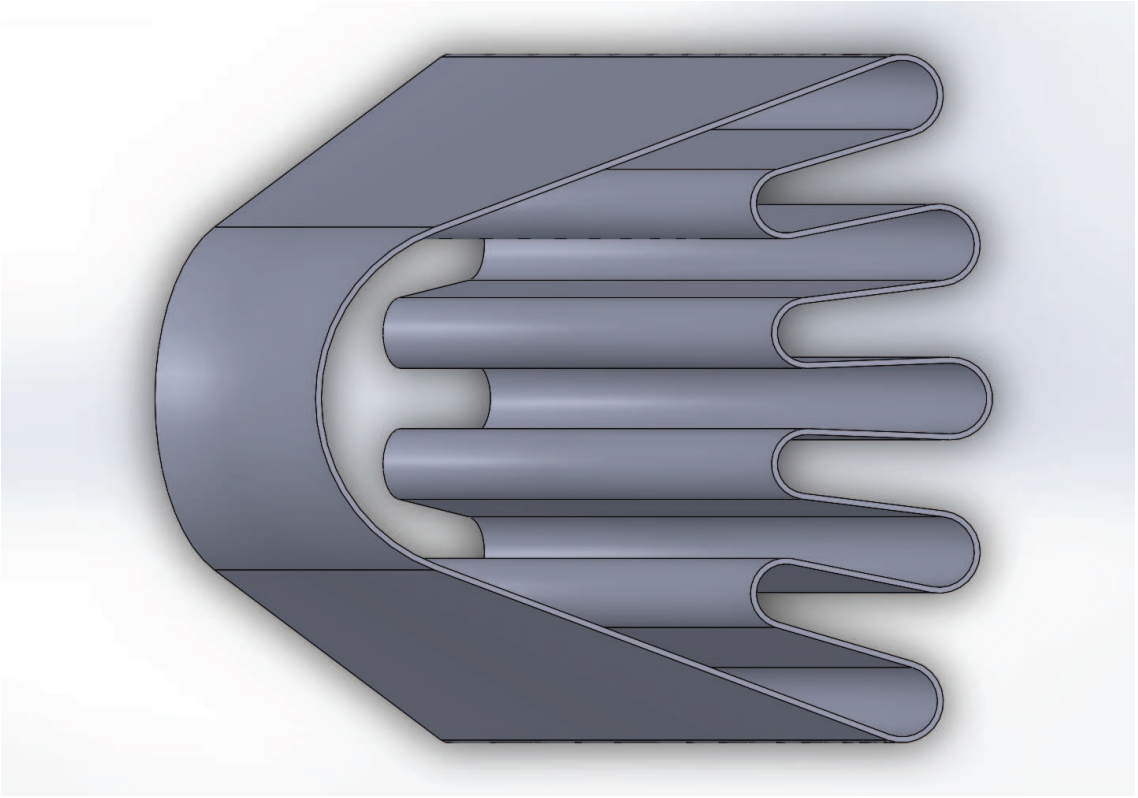

Figure C.4: Step 8.

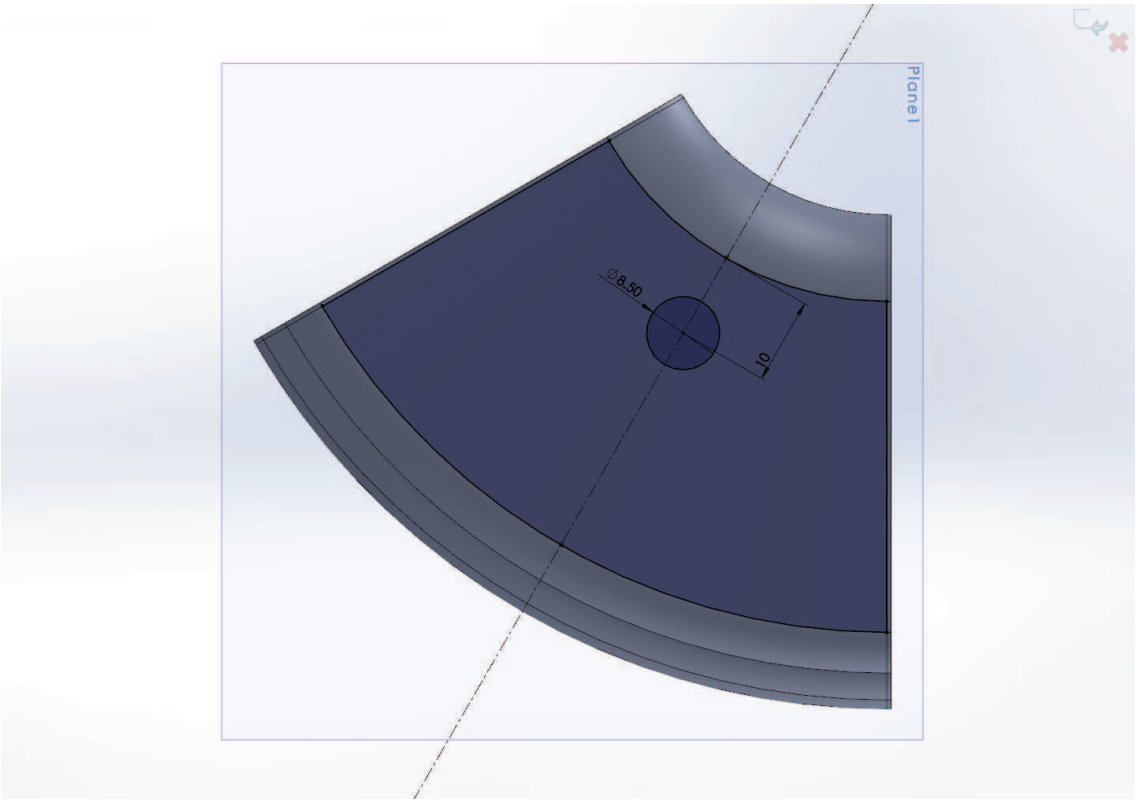

Figure C.5: Step 13.

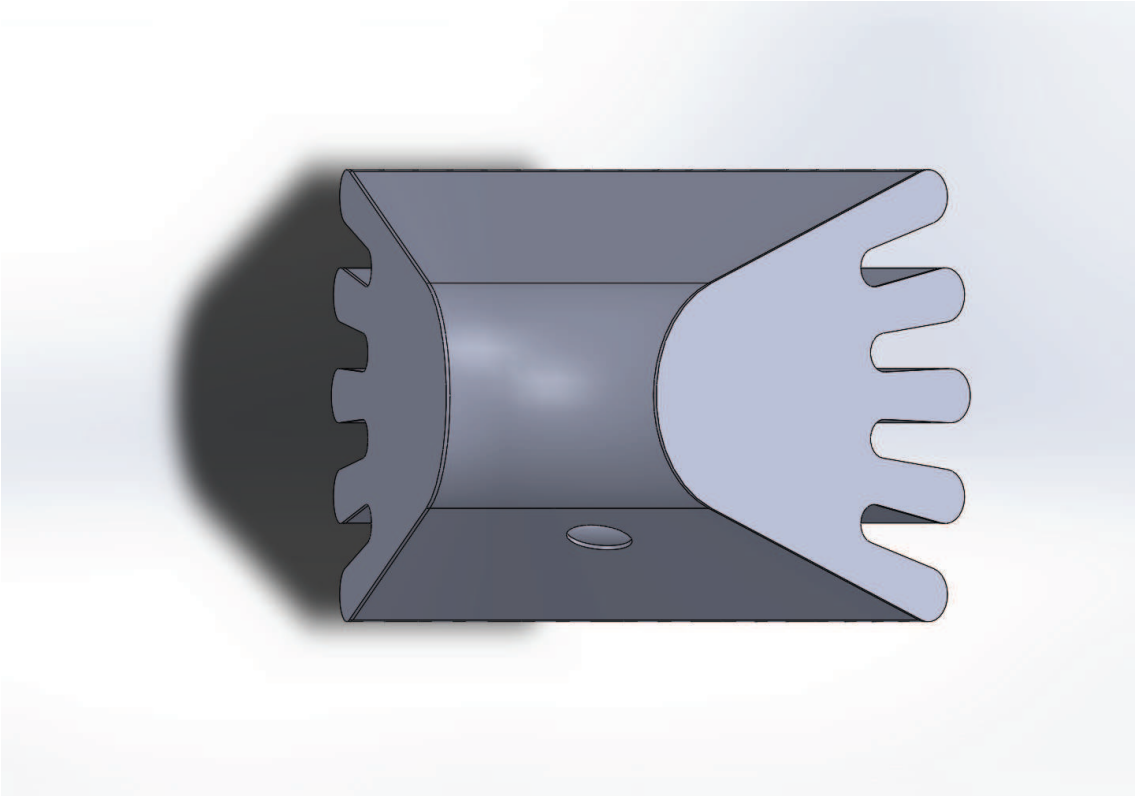

Figure C.6: CAD model of the soft inflatable rotary actuator with flat sides.

Appendix D

Designing a Soft Inflatable Rotary Actuator with Lofted Sides in SOLIDWORKS

From Section 4.1, it was known that the sides of the soft inflatable rotary actuator have to be made compliant in order to facilitate its deflection on the primary face. As such, two mechanical designs of the sides were explored, namely, the flat sides and the lofted sides.

Lofted sides derive their name from the tool that they are created from, namely the Surface Loft tool. As compared to the flat sides, these sides protrude out of the plane and have folds integrated into them. This was done to increase the internal surface area and hence, the compliance of the sides. Creating them in SOLIDWORKS is significantly more difficult than the above, and it is one of the main contributions of this report. In the following, the procedure to generate the CAD of a soft inflatable rotary actuator with lofted sides is described:

1. Open SOLIDWORKS and create a new part file.
2. Select the top plane and create a new sketch.
3. Sketch the following guides: i) An infinite vertical line that intersects with the origin. ii) An infinite horizontal line that intersects with the origin. iii) Three circles to guide the U-Shaped geometry. For this example, the following diameters were used $D = \{138, 150, 162\}$mm. These diameters indicate that a modified U-shaped geometry is being used. Using the wave analogy for the sake of simplicity, $h = 12.0$mm is used to define both the positive and negative amplitudes (note that this is different from the original U-shaped geometry as shown in Fig. 3.1, where b is used to define the negative amplitude).
4. Follow the sketch, as shown in Fig. D.1. Do note that $b = 3.00$mm, the guidelines intersect the origin as well as are tangent to the circles and that the lines which connect the circles are collinear with the guidelines. The number of folds drawn was arbitrarily chosen to keep the size of the actuator small.
5. By using the Trim Entities tool, delete the lines that are not needed as shown in Fig. D.2.
6. By using the Mirror Entities tool, reflect the sketch about the horizontal line and fillet the lines which intersect at the origin. A fillet of 15.0mm was also arbitrarily chosen. The sketch, as shown in Fig. D.3 should be obtained.
7. Create a new sketch on the top plane.

8. Select the previous sketch and use the Convert Entities tool to obtain a copy of the previous sketch.
9. Repeat Steps 7 and 8 to obtain one copy of the sketch.
10. Delete the necessary lines in the two sketch copies to obtain Fig. D.4 and Fig. D.5.
11. Create a sketch on the front plane and create a spline with the following dimensions, as shown in Fig. D.6. Ensure that the spline pierces the midpoint of the two previous sketches.
12. Using the Surface Loft tool (Insert > Surface > Loft), follow the settings as shown in Fig. D.7.
13. Create a new sketch on the top plane and draw a line, as shown in Fig. D.8.
14. Using the Boundary Surface tool (Insert > Surface > Boundary Surface), a surface is created to cap the surface from the top. This is as shown in Fig. D.9.
15. Using the Mirror tool, make a copy of this surface for the bottom side of the surface.
16. Knit the surfaces together (Insert > Surface > Knit) to form a single surface.
17. This surface is then thickened to the desired value of 0.50mm (Insert > Boss/Base > Thicken). However should the surface be unable to thicken, it means either of two things. The thickened surfaces could either be intersecting one another or are too close to one another. Make the necessary changes depending on the situation. The part, as shown in Fig. D.10 should be obtained.
18. Make a sketch and use the Extrude Cut tool to cut the part into half, as shown in Fig. D.11. This is done to simplify the part as it is symmetrical as well as to avoid any bugs in SOLIDWORKS.
19. As a result of using the Surface Loft and Thicken tools, the part created has an uneven surface. SOLIDWORKS is unable to work with this kind of surface. Hence, using the Extrude Cut tool, shave 1.00mm off the part and ensure to keep the correct portion of the part. This is shown in Fig. D.12.
20. The removed material is now replaced with a flat extrusion. To do this, create a sketch on the now flat surface and extrude its outline by 1.00mm. This involves the Convert Entities, Extrude Boss/Base tools. The result of this step is as shown in Fig. D.13.
21. Using the Mirror tool, reflect this part about the front plane. The result of this step is as shown in Fig. D.14.
22. Create a sketch of the flat side of the part.
23. Using the Revolve Boss/Base tool, revolve the part to the desired amount. For this example, 30° was chosen. The result of this step is as shown in Fig. D.15.
24. Create a plane (Insert > Reference Geometry > Plane) on the flat surface of the revolved section of the part.
25. Using the Mirror tool, reflect the part about this plane. The result of this step is as shown in Fig. D.16.
26. Create another plane. Select the front plane as the reference and offset it by 30.0mm.
27. Select the plane and follow the sketch, as shown in Fig. D.17. The circle here is used to cut the hole for the flange.
28. Using the Extrude Cut tool, cut the hole into the bottom side of the part.

With these steps, the CAD model of the soft inflatable rotary actuator with lofted sides is completed, as shown in Fig. D.18.

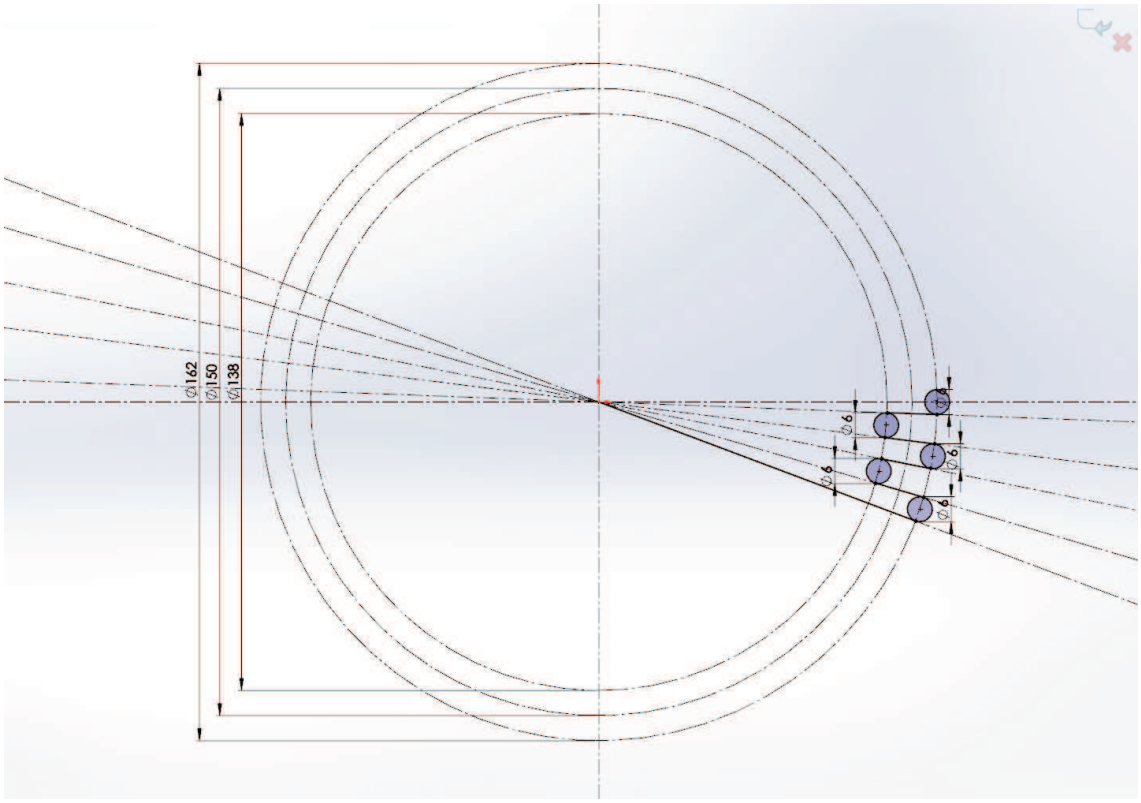

Figure D.1: Step 4.

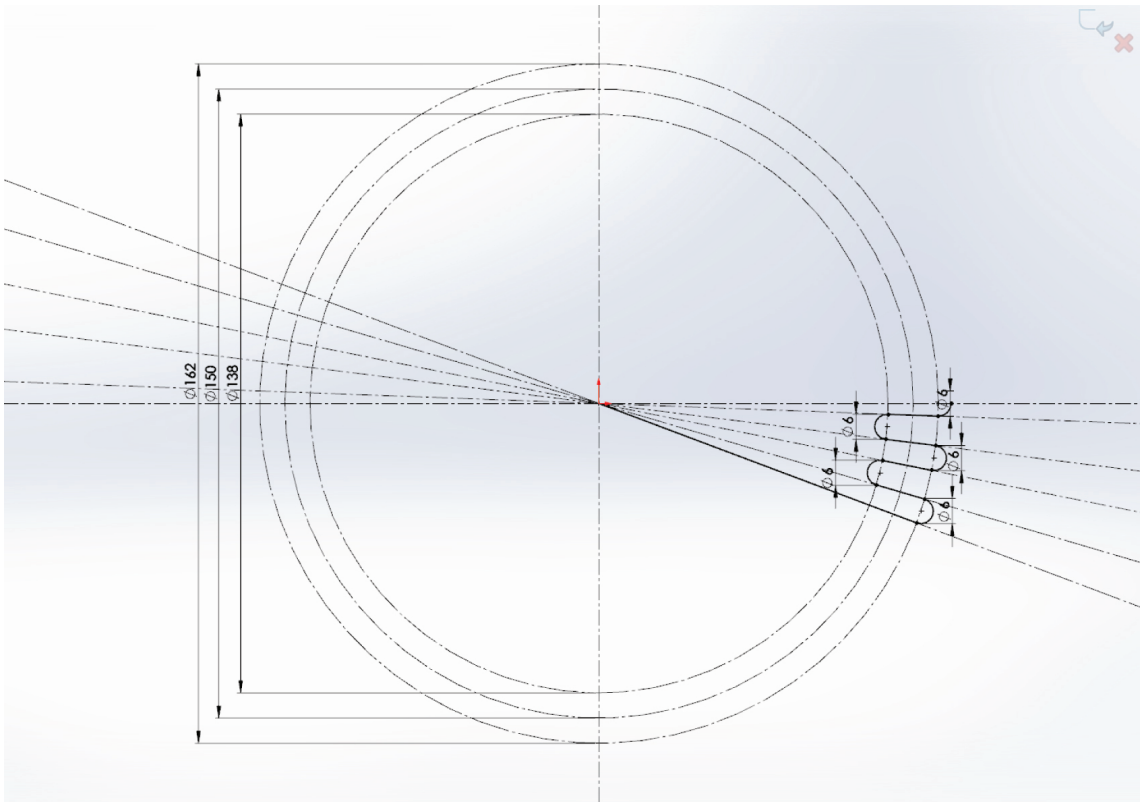

Figure D.2: Step 5.

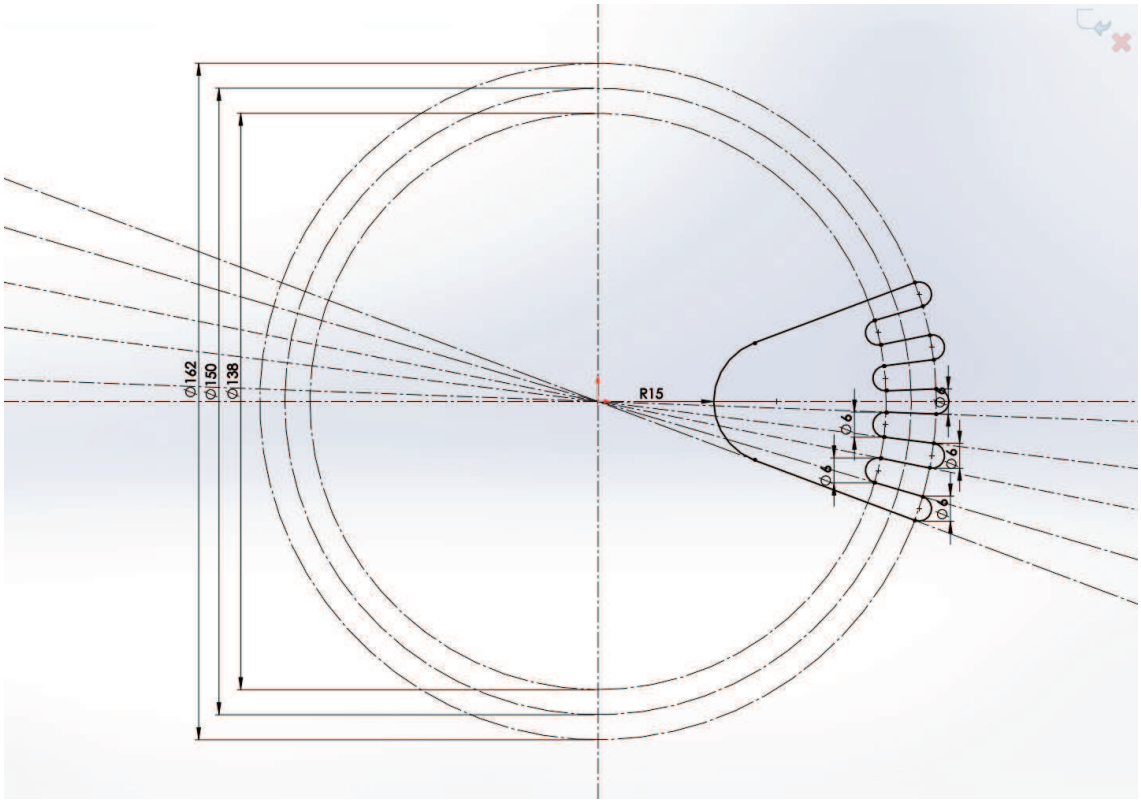

Figure D.3: Step 6.

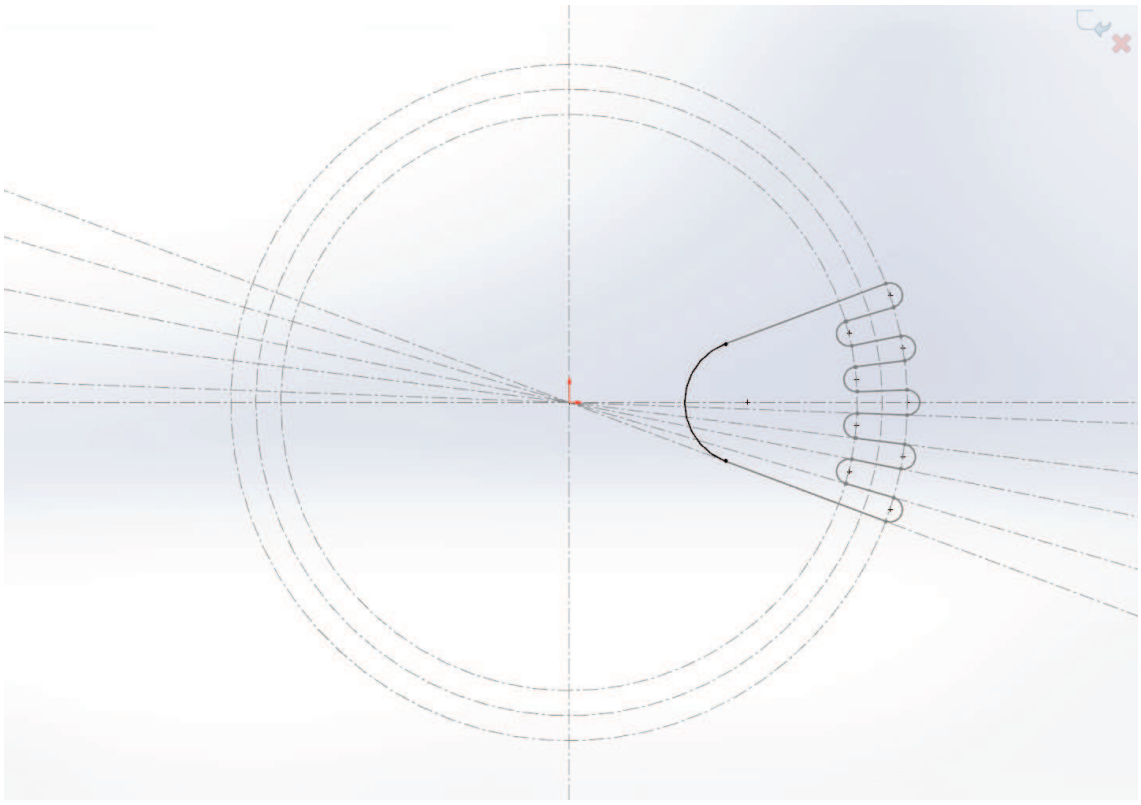

Figure D.4: Step 10.

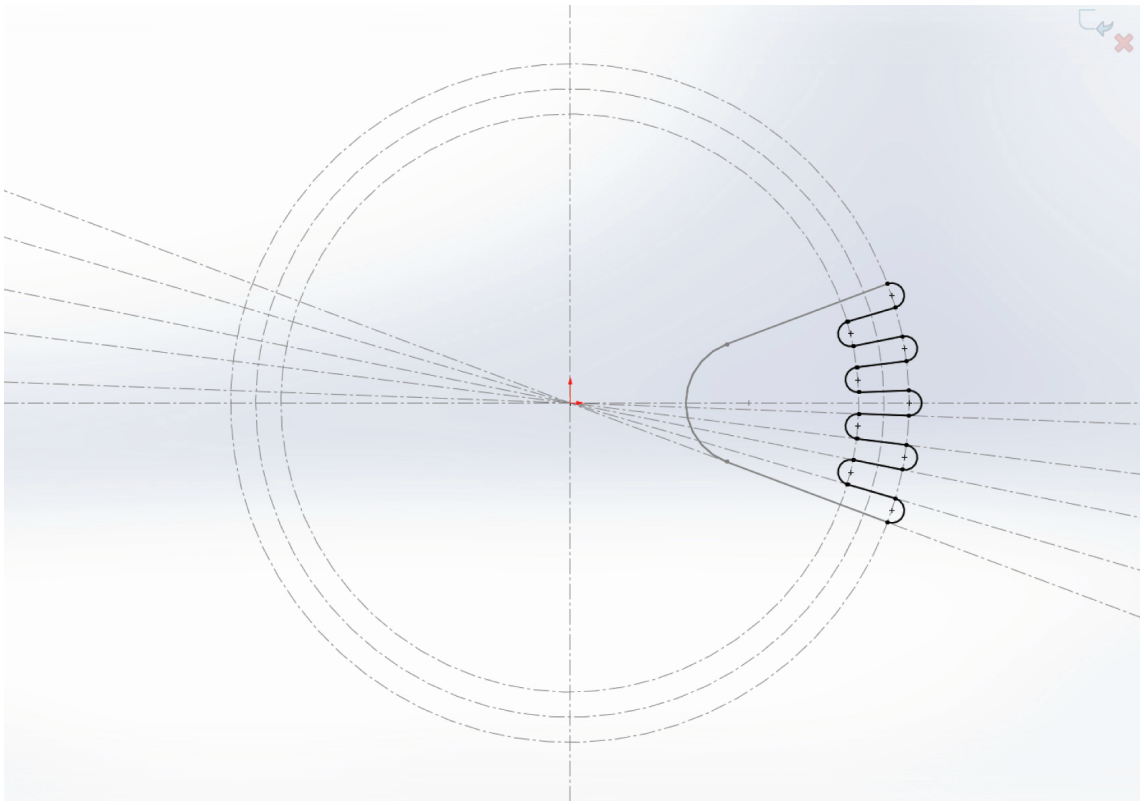

Figure D.5: Step 10.

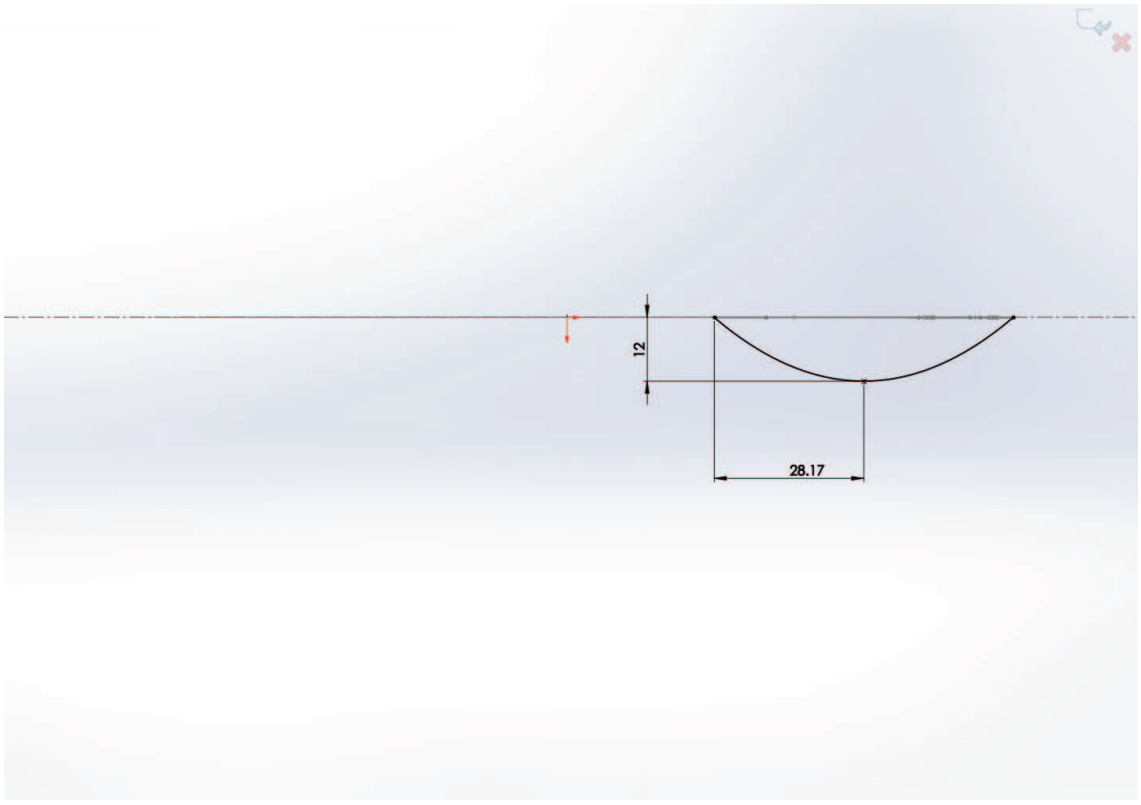

Figure D.6: Step 11.

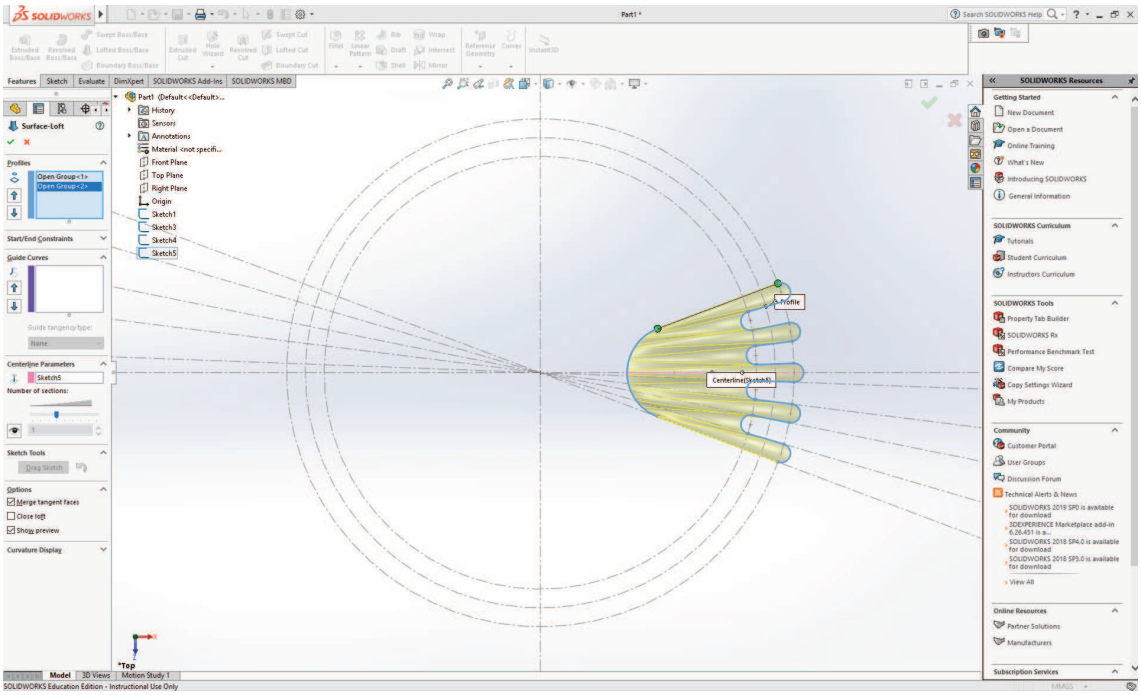

Figure D.7: Step 12.

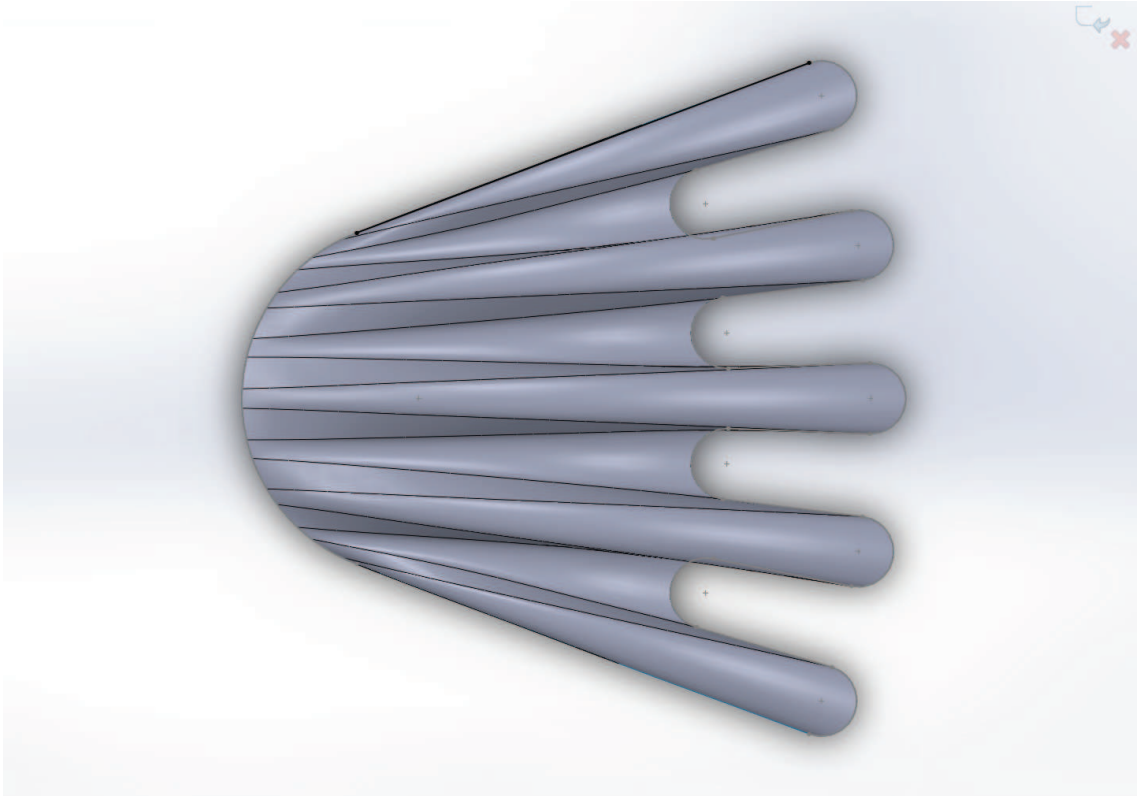

Figure D.8: Step 13.

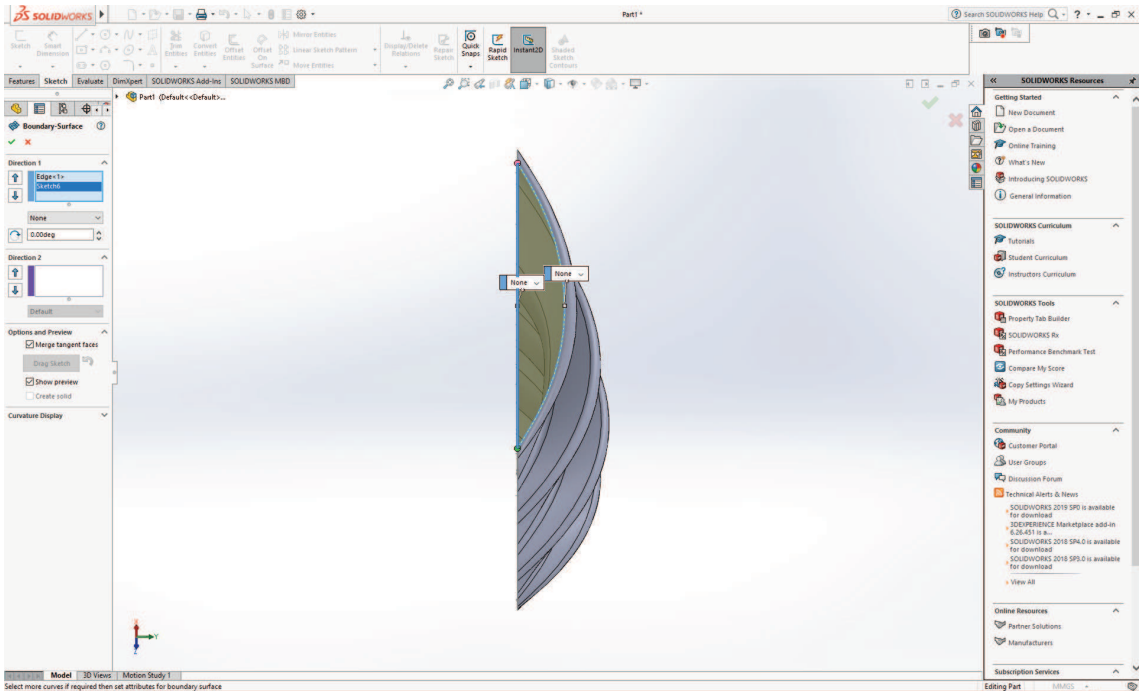

Figure D.9: Step 14.

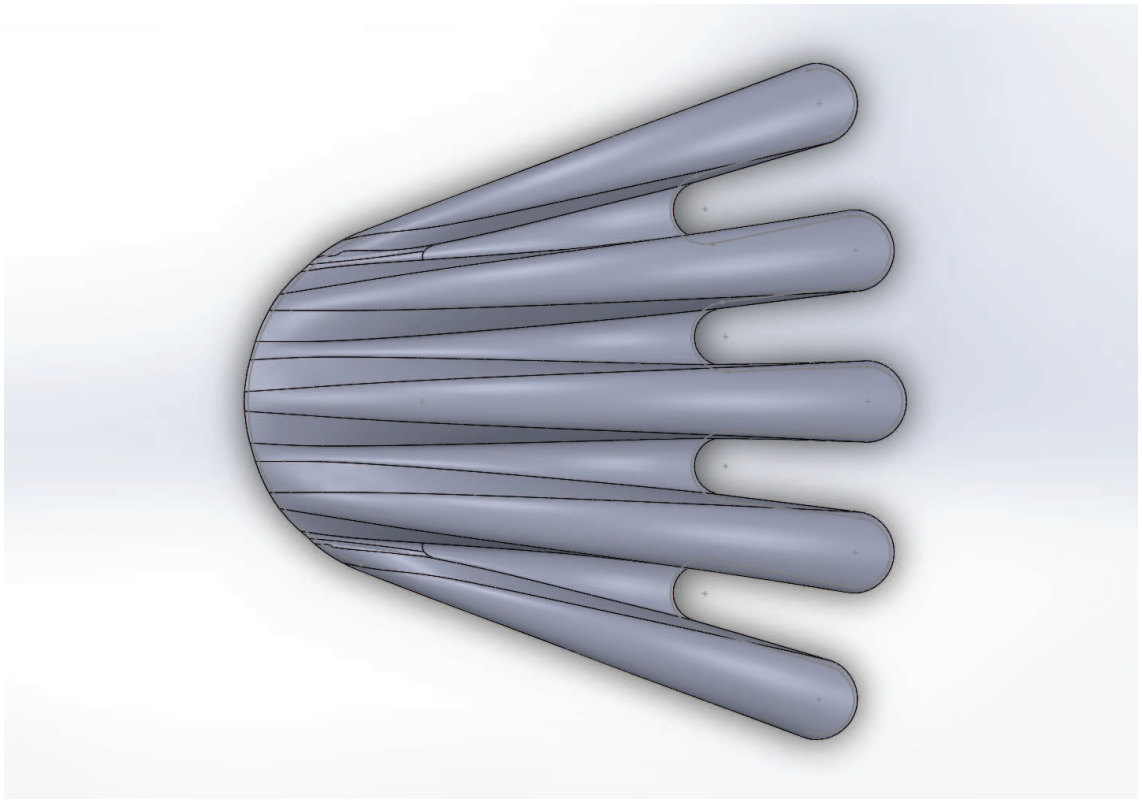

Figure D.10: Step 17.

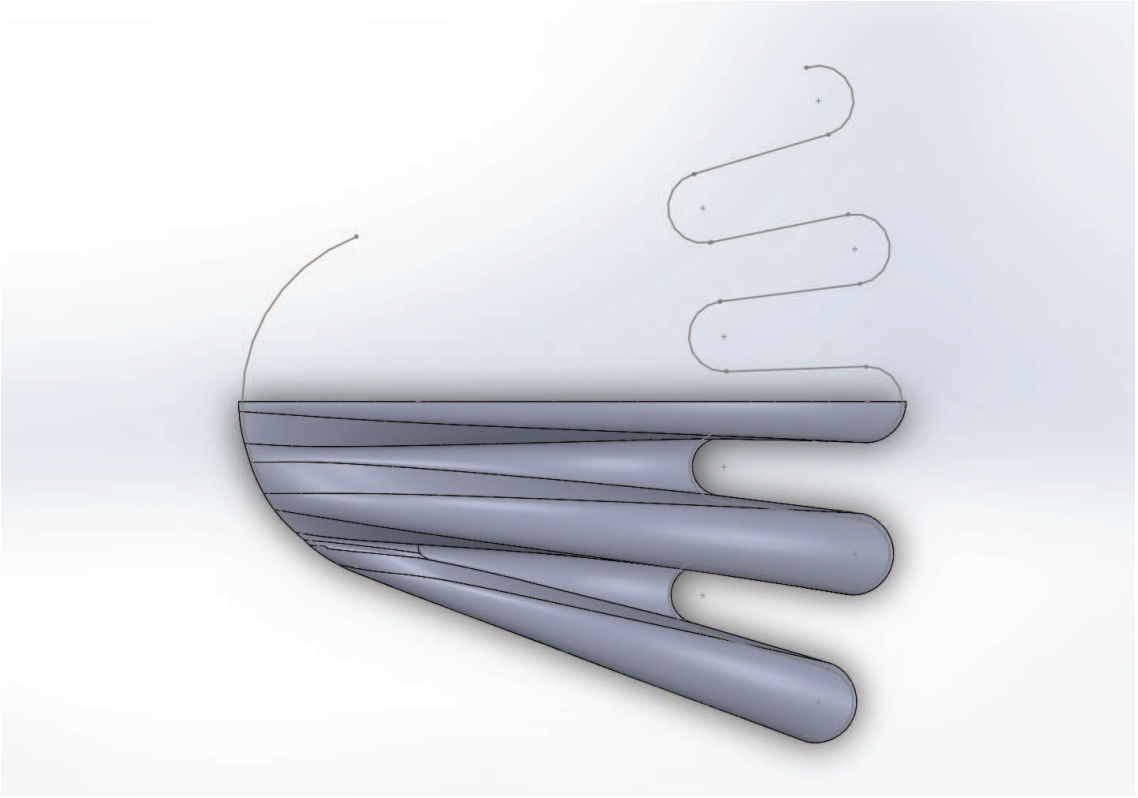

Figure D.11: Step 18.

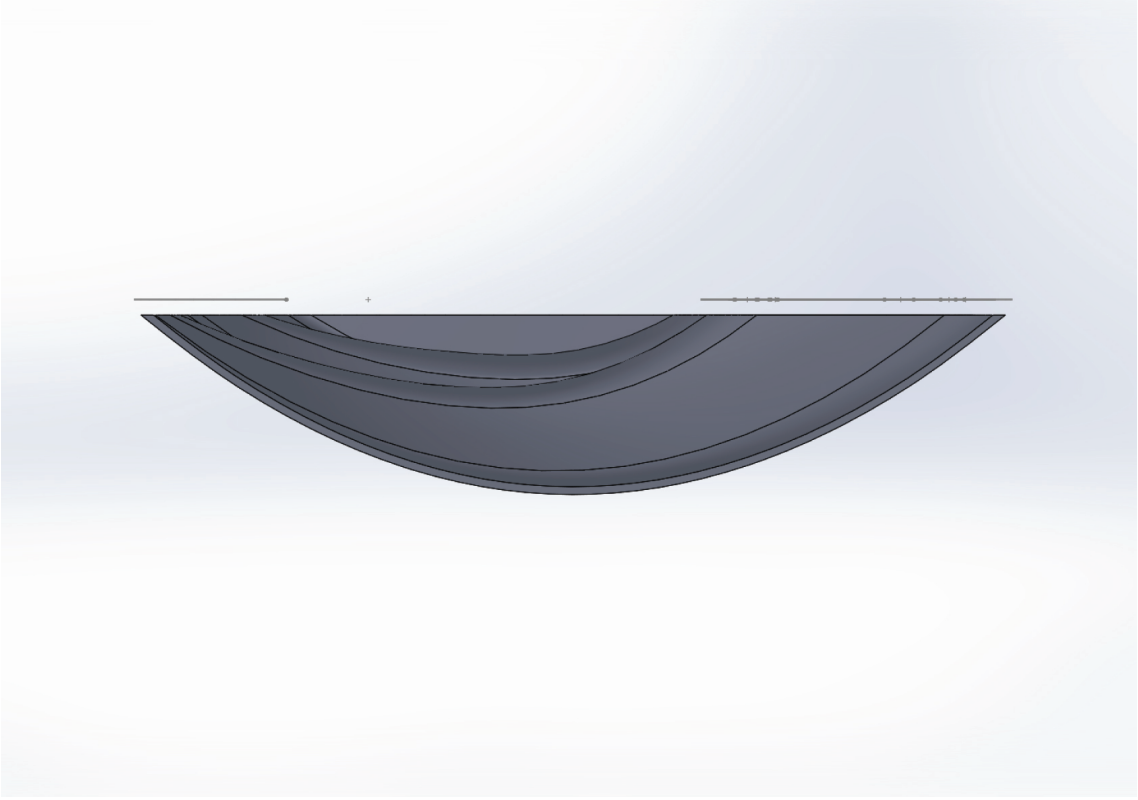

Figure D.12: Step 19.

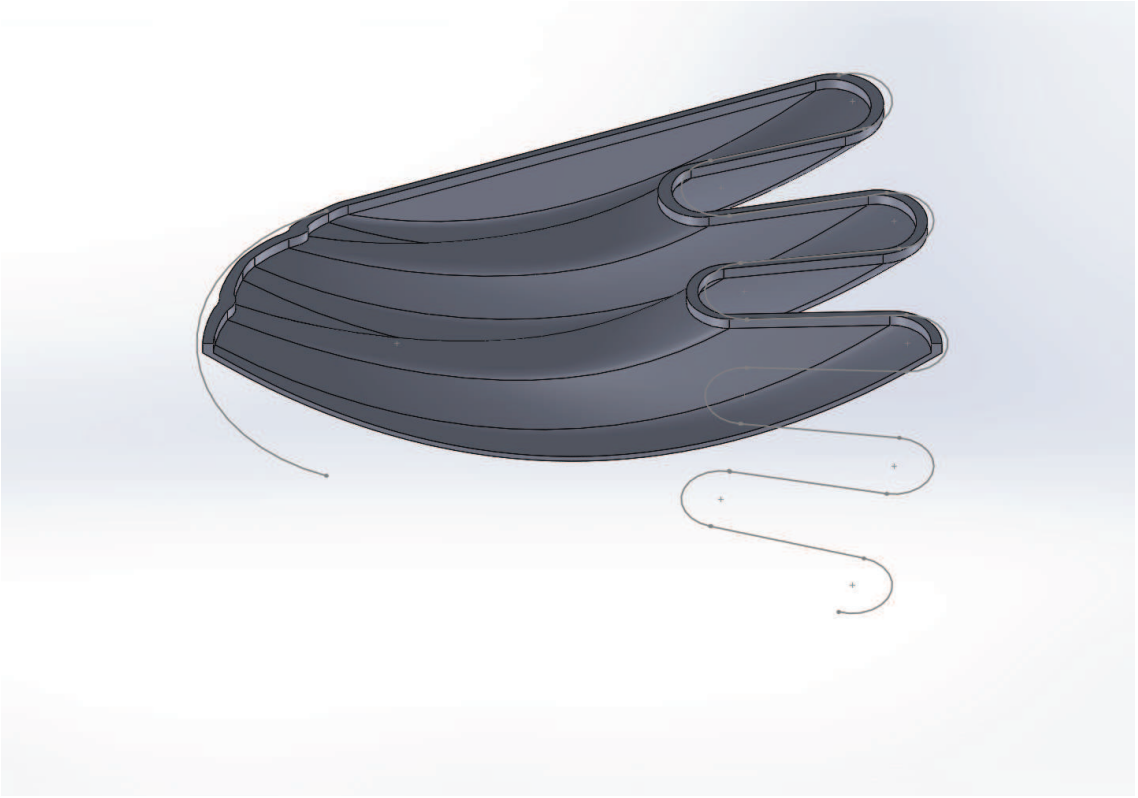

Figure D.13: Step 20.

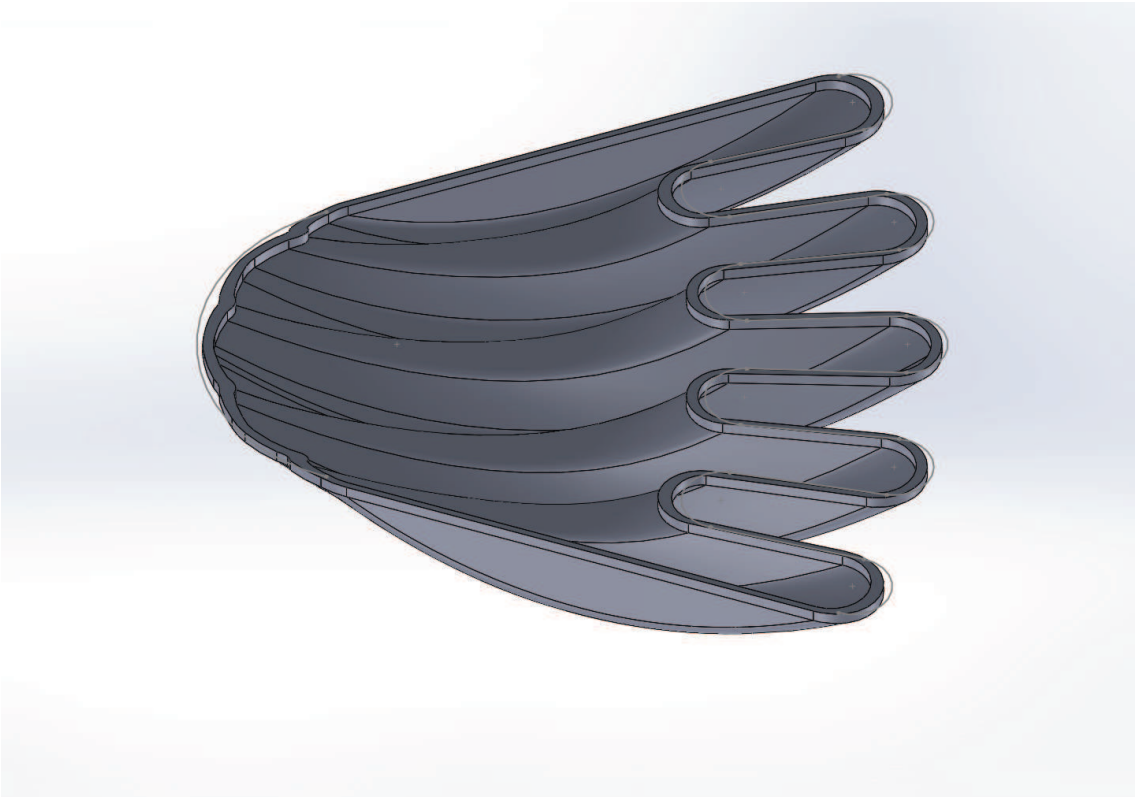

Figure D.14: Step 21.

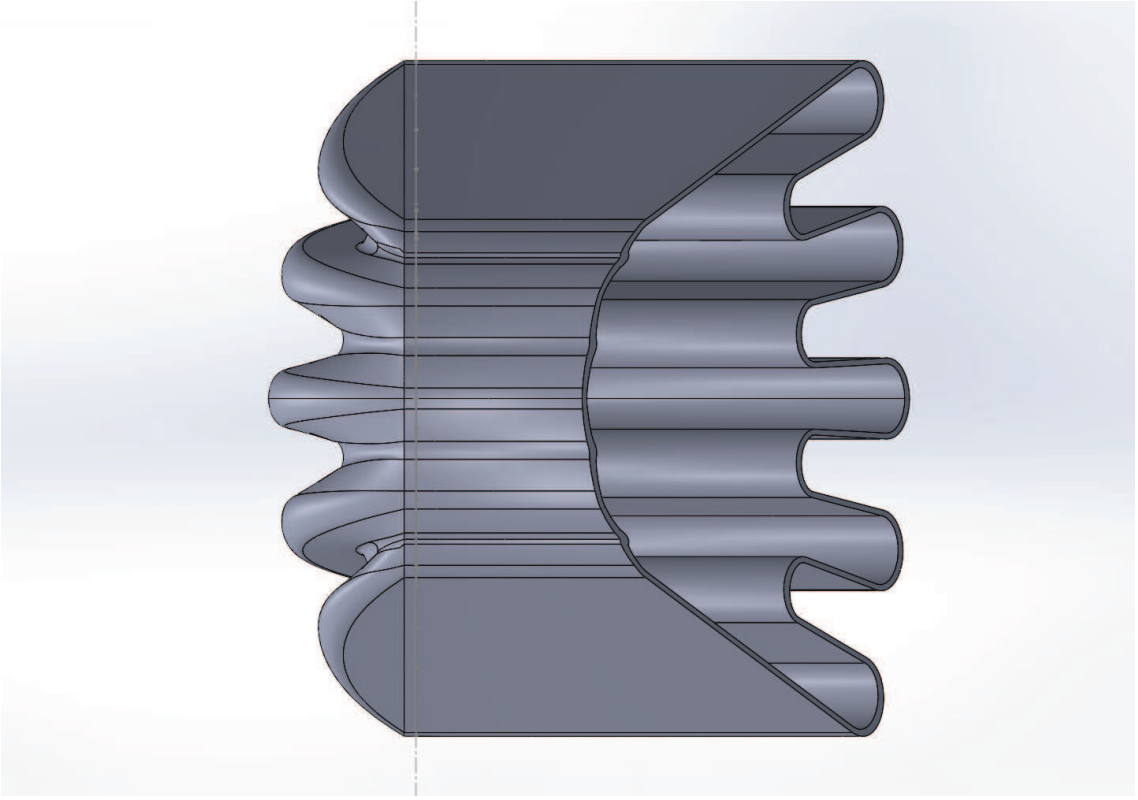

Figure D.15: Step 23.

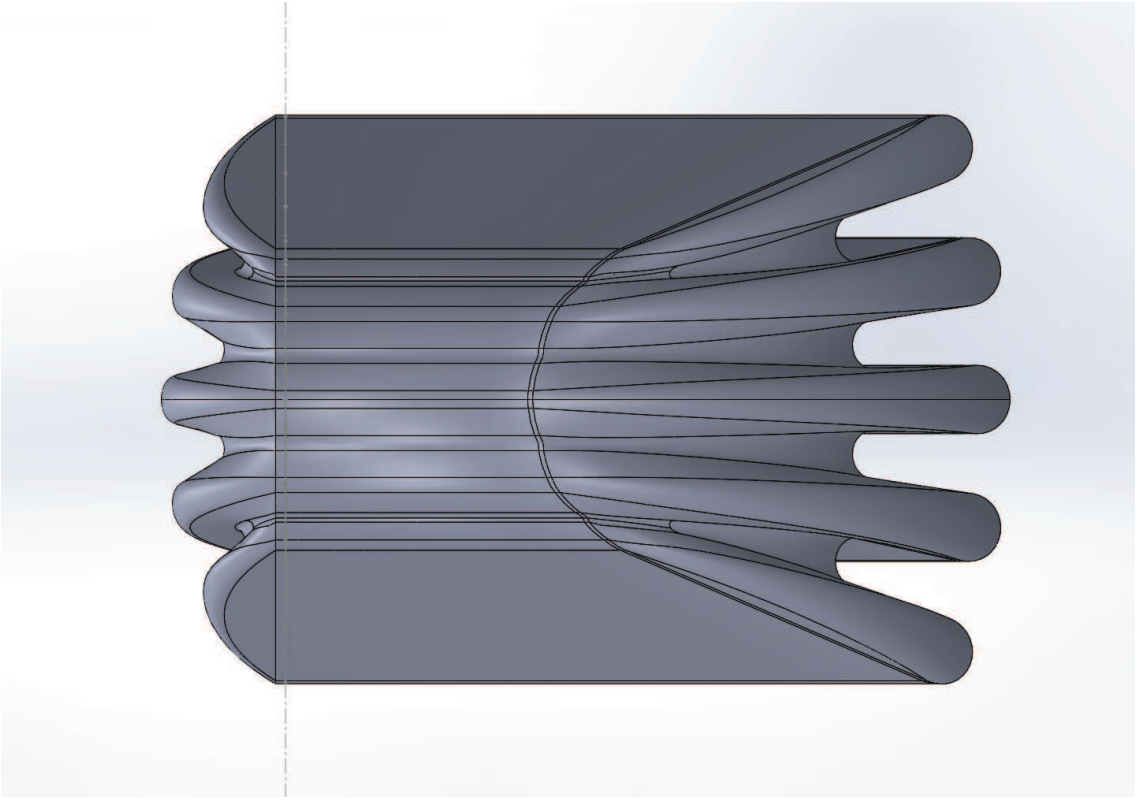

Figure D.16: Step 25.

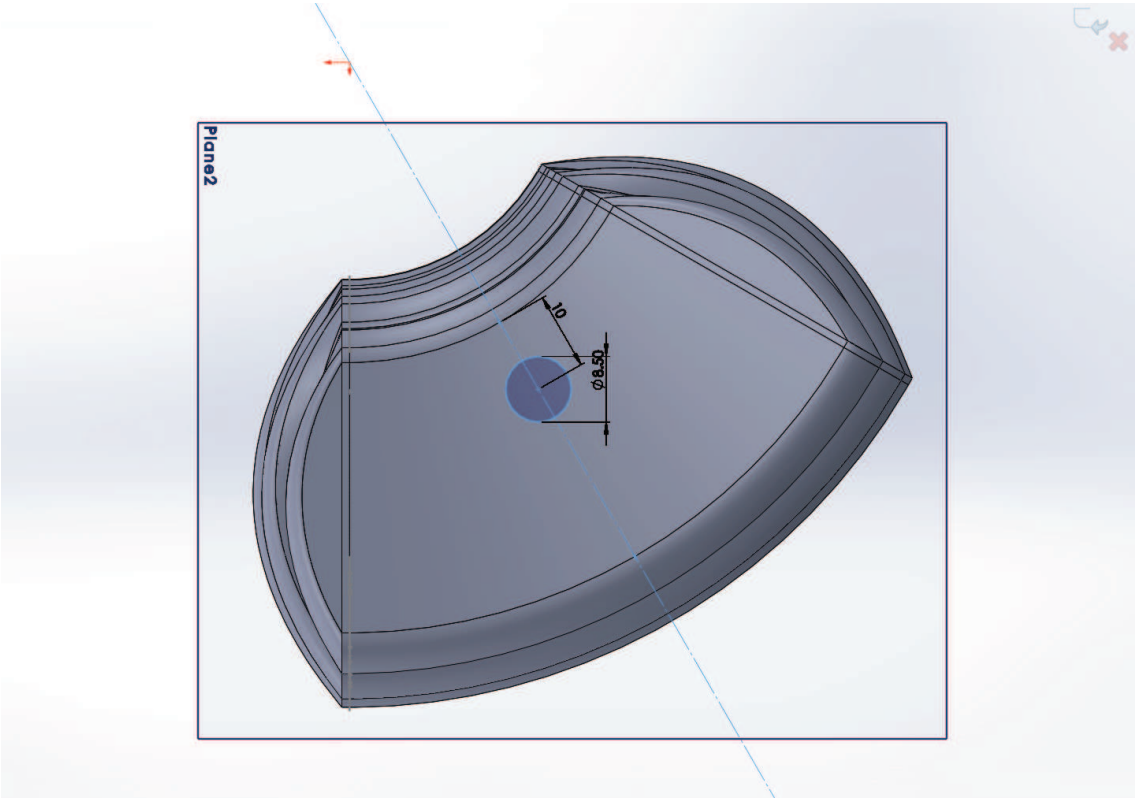

Figure D.17: Step 27.

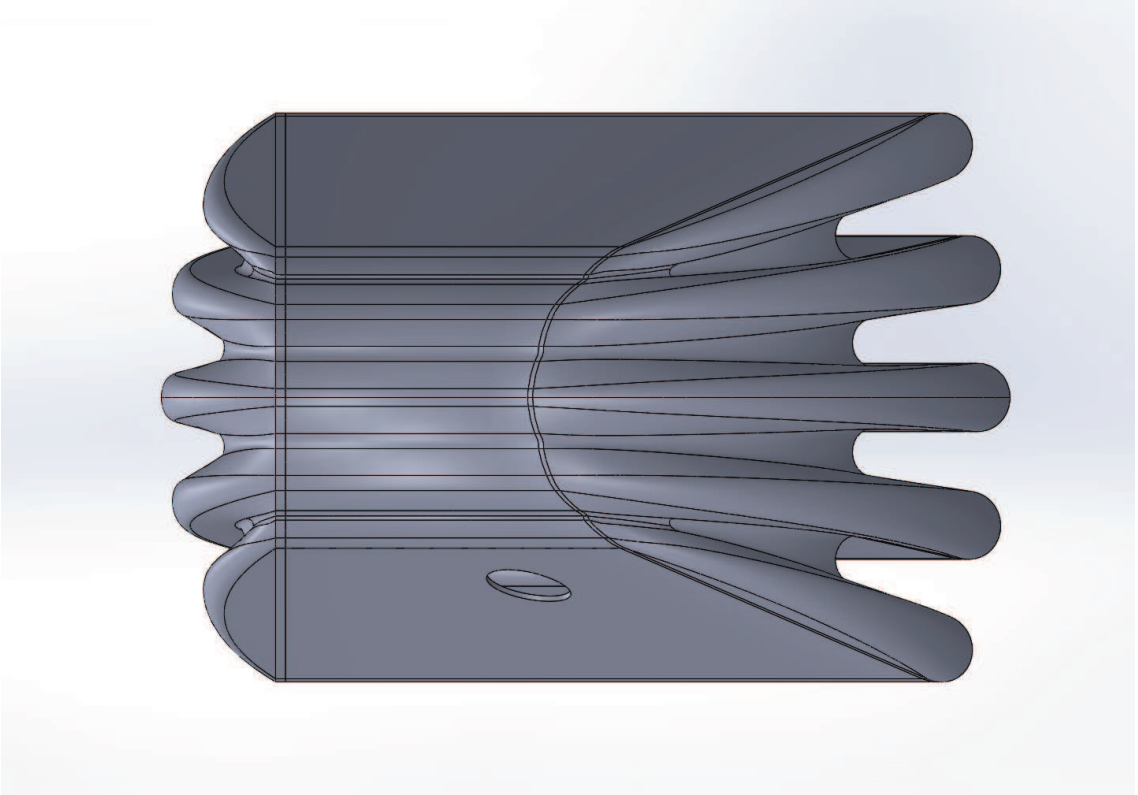

Figure D.18: CAD model of the soft inflatable rotary actuator with lofted sides.

Bibliography

[1] B. Gorissen, D. Reynaerts, S. Konishi, K. Yoshida, J. Kim, and M. De Volder, "Elastic inflatable actuators for soft robotic applications," *Advanced Materials*, vol. 29, no. 43, 2017.

[2] S. Kim, C. Laschi, and B. Trimmer, "Soft robotics: a bioinspired evolution in robotics," *Trends in Biotechnology*, vol. 29, no. 43, pp. 287–294, 2013.

[3] B. Mosadegh, P. Polygerinos, C. Keplinger, S. Wennstedt, R. Shepard, U. Gupta, J. Shim, K. Bertoldi, C. Walsh, and G. Whitesides, "Pneumatic networks for soft robotics that actuate quickly," *Functional Materials*, vol. 24, no. 15, pp. 2163–2170, 2014.

[4] H.-K. Yap, F. Sebastian, C. Wiedeman, and C.-H. Yeow, "Design and characterization of low-cost fabric-based flat pneumatic actuators for soft assistive glove application," in *IEEE International Conference on Rehabilitation Robotics*, 2017.

[5] M. Hofer and R. D'Andrea, "Design, modeling and control of a soft robotic arm," in *IEEE/RSJ International Conference on Intelligent Robotics*, 2018.

[6] G. A. Pratt and M. M. Williamson, "Series elastic actuators," in *IEEE/RSJ International Conference on Intelligent Robots and Systems*, 1995, pp. 399–406.

[7] R. Van Ham, T. G. Sugar, B. Vanderborght, K. W. Hollander, and D. Lefeber, "Compliant actuator designs," *IEEE Robotics & Automation Magazine*, vol. 16, no. 3, pp. 81–94, 2009.

[8] Y. Sun, Y.-S. Song, and J. Paik, "Characterization of silicone rubber based soft pneumatic actuators," in *IEEE/RSJ International Conference on Intelligent Robotics*, 2013, pp. 4446–4453.

[9] X. Wang, M. Jiang, Z. Zhou, J. Gou, and D. Hui, "3d printing of polymer matrix composites: A review and prospective," *Composites Part B: Engineering*, vol. 110, pp. 442–458, 2017.

[10] *HP 3D High Reusability PA 12*, HP Development Company, 2017.

[11] *Agilus30*, Stratasys Ltd., 2017.

[12] J. Wilson, "Mechanics of bellows: A critical survey," *International Journal of Mechanical Sciences*, vol. 26, pp. 593–605, 1984.

ETH
Eidgenössische Technische Hochschule Zürich
Swiss Federal Institute of Technology Zurich

Institute for Dynamic Systems and Control
Prof. Dr. R. D'Andrea, Prof. Dr. E. Frazzoli, Prof. Dr. C. Onder, Prof. Dr. M. Zeilinger

Title of work:

3D-Printed Inflatable Actuators

Design and Development of Soft Actuators for a Pneumatically-Actuated Soft Robotic Arm

Thesis type and date:

Semester Project, August 2019

Supervision:

Matthias Hofer
Prof. Dr. Raffaello D'Andrea

Student:

Name: Hong Fai Lau
E-mail: lauh@student.ethz.ch
Legi-Nr.: 17-937-707
Semester: Fall 2018

Statement regarding plagiarism:

By signing this statement, I affirm that I have read and signed the Declaration of Originality, independently produced this paper, and adhered to the general practice of source citation in this subject-area.

Declaration of Originality:

`https://www.ethz.ch/content/dam/ethz/main/education/rechtliches-abschluesse/leistungskontrollen/declaration-originality.pdf`

Zurich, 4.8.2019: